JOC Article
pubs.acs.org/joc

# Synthesis of 2′,4′-Propylene-Bridged (Carba-ENA) Thymidine and Its Analogues: The Engineering of Electrostatic and Steric Effects at the Bottom of the Minor Groove for Nuclease and Thermodynamic Stabilities and Elicitation of RNase H

Yi Liu, Jianfeng Xu, Mansoureh Karimiahmadabadi, Chuanzheng Zhou, and Jyoti Chattopadhyaya*

*Bioorganic Chemistry Program, Department of Cell and Molecular Biology, Box 581, Biomedical Center, Uppsala University, SE-751 23 Uppsala, Sweden*

*jyoti@boc.uu.se*

*Received June 21, 2010*

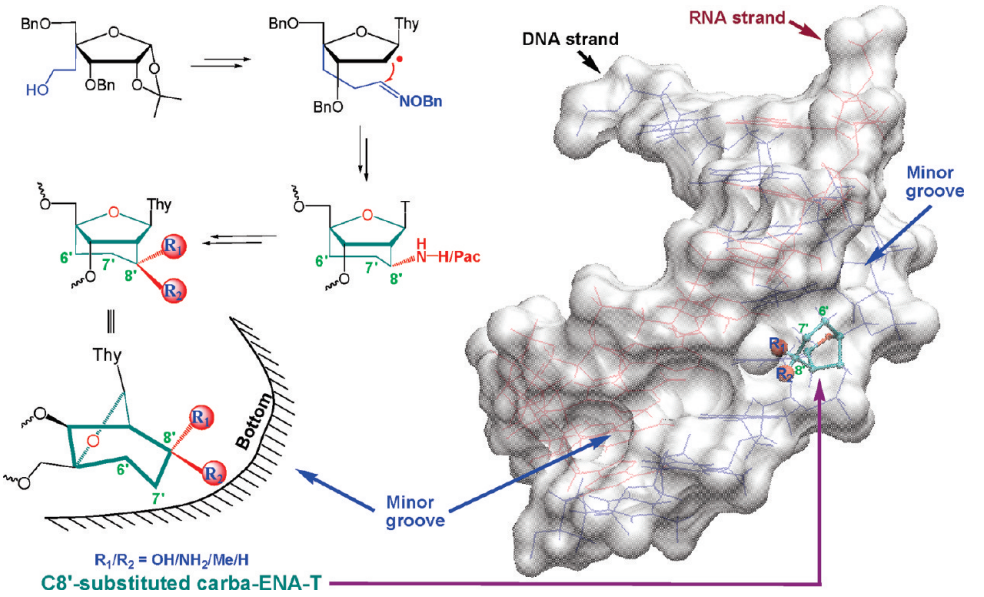


2′,4′-Propylene-bridged thymidine (carba-ENA-T) and five 8′-Me/$NH_2$/OH modified carba-ENA-T analogues have been prepared through intramolecular radical addition to C=N of the tethered oxime-ether. These carba-ENA nucleosides have been subsequently incorporated into 15mer oligodeoxynucleotides (AON), and their affinity toward cDNA and RNA, nuclease resistance, and RNase H recruitment capability have been investigated in comparison with those of the native and ENA counterparts. These carba-ENAs modified AONs are highly RNA-selective since all of them led to slight thermal stabilization effect for the AON:RNA duplex, but quite large destabilization effect for the AON:DNA duplex. It was found that different C8′ substituents (at the bottom of the minor groove) on carba-ENA-T only led to rather small variation of thermal stability of the AON:RNA duplexes. We, however, observed that the parent carba-ENA-T modified AONs exhibited higher nucleolytic stability than those of the ENA-T modified counterparts. The nucleolytic stability of carba-ENA-T modified AONs can be further modulated by C8′ substituent to variable extents depending on not only the chemical nature but also the stereochemical orientation of the C8′ substituents: Thus, (1) 8′*S*-Me on carba-ENA increases the nucleolytic stability but 8′*R*-Me leads to a decreased effect; (2) 8′*R*-OH on carba-ENA had little, if any, effect on nuclease resistance but 8′*S*-OH resulted in significantly decreased nucleolytic stability; and (3) 8′-$NH_2$ substituted carba-ENA leads to obvious loss in the nuclease resistance. The RNA strand in all of the carba-ENA derivatives modified AON:RNA hybrid duplexes can be digested by RNase H1 with high efficiency, even at twice the rate of those of the native and ENA modified counterpart.


Published on Web 10/07/2010 DOI: 10.1021/jo101207d

## Introduction

Oligonucleotides with high affinity and specificity toward complementary DNA or RNA through Watson−Crick hybridization can be potentially used as diagnostic and therapeutic agents via several different machineries, such as antisense,[1] ribozymes,[2] small interfering RNA (siRNA),[3] microRNA (miRNA),[4] and triple helix-forming oligonucleotides (TFOs).[5] In the past two decades, the effort to develop AON with striking target affinity and biological stability has resulted in the synthesis of a large number of chemically modified nucleotides, among which the locked nucleic acid (LNA) has attracted extensive attention.[6] The 2′,4′-linkage in LNA is able to lock the conformation of the sugar moiety into a perfect *N*-type conformation.[7] When LNA monomer was incorporated into oligonucleotide, it can spontaneously tune its neighboring natural nucleotides from *S*- to *N*-conformation, resulting in an A-type or A-type-like duplex form consistent with the predominant form of the RNA helix.[8] Hence, LNA-modified AONs exhibit remarkable sequence selectivity for the complementary RNA over the DNA.[6]

Though the striking feature of LNA-modified oligos has given immense opportunity to a broad application in biotechnology and therapeutics,[9] it is clear that further development is required, due to the low nuclease resistance and hepatotoxicity of LNA.[10,11] Thus large numbers of chemically modified analogues with 2′,4′-linkage have been designed and synthesized.[12] Some of the modifications focus on introduction of different functions at the C6′ in LNA. For example, Nielsen[13] and Swayze[14] have independently reported C6′-$CH_2$OH-LNA and C6′-Me-LNA (cEt), C6′-$CH_2$OMe-LNA (cMOE), respectively. The cEt and cMOE modified oligonucleotides showed improved exonucleolytic resistance without loss of hybridization behavior compared to the LNA-modified counterpart. Another type of modification focuses on expanding ring size or introducing heteroatoms into different positions on the locked ring moiety, such as ENA,[11] aza-ENA,[15] PrNA,[11] BNA$^{COC}$,[16] and BNA$^{NC}$.[17]

Replacement of the 2′-*O*- in LNA with 2′-$CH_2$- results in a more hydrophobically locked carba-LNA nucleoside, which has been synthesized recently by us through a radical cyclization strategy.[18−20] The advantage of carba-LNA is that carba-LNA-modified AONs exhibit similar hybridizing ability for the complementary RNA as that of LNA counterparts, but the former showed significantly improved nucleolytic resistance than the latter. Moreover, we found that the nucleolytic resistance and hybridizing ability of carba-LNA can be finely modulated by introduction of hydrophobic methyl, hydrophilic hydroxyl, or zwitterionic amino functions at C6′ and/or C7′ of the carbocyclic moiety. This modulation was found to be greatly dependent on not only the nature but also the steric orientation of the substituents at the chiral C6′ and/or C7′ position of the carbocyclic moiety in the carba-LNA.

Carba-ENA that contains a 2′,4′-propyl linkage has also been synthesized by us through a radical cyclization reaction[21] and also independently by Nielsen's group through a ring-closing metathesis.[22,23] Compared with carba-LNA, carba-ENA has a sterically larger and more hydrophobically carbocyclic linkage. This structural feature has rendered carba-ENA incorporated oligos with more improved nucleolytic resistance than those of carba-LNA counterparts. However, none of these works reported any studies on the nuclease stability of parent carba-ENA-modified AONs. In the present study, we report a new synthetic strategy for carba-ENA-T and study the nucleolytic stability as well as other antisense properties of carba-ENA-modified AONs.

In addition, C6′- and/or C7′-substitued carba-ENA analogues have been synthesized by Nielsen's group[23] and us[18] independently. Our work showed that the C6′ substituent on carba-ENA exerted a significant effect on nucleolytic stability and the effect depends on the nature of the substituents. Nielsen's work showed hydrophilic substituents at C6′ and/or C7′ led to increased affinity for complementary RNA and DNA. Compared to C6′ and C7′ substituents on carba-ENA, the C8′ substituent should be more interesting because a C8′ substituent is located at the bottom of the minor groove, hence it should have a larger effect on thermodynamic stability and other properties of AON:RNA and AON:DNA duplexes. In this report, we also describe the synthesis of 8′-$NH_2$/OH/Me-substituted carba-ENA analogues in detail. Biophysical and biological properties such as target affinity toward complementary DNA and RNA, nucleolytic stability, and the RNase H recruitment capability of AONs with these 8′-substituted carba-ENAs modifications have been tested and

(1) (a) Bennett, C. F.; Swayze, E. E. *Annu. Rev. Pharmacol. Toxicol.* **2010**, *50*, 259–293. (b) Uhlman, E; Peyman, A. *Chem. Rev.* **1990**, *90*, 543–584.
(2) Schubert, S.; Kurreck, J. *Curr. Drug Targets* **2004**, *5*, 667–681.
(3) de Fougerolles, A.; Vornlocher, H. P.; Maraganore, J.; Lieberman, J. *Nat. Rev. Drug Discovery* **2007**, *6*, 443–453.
(4) Bartel, D. P. *Cell* **2004**, *116*, 281–297.
(5) Buchini, S.; Leumann, C. J. *Curr. Opin. Chem. Biol.* **2003**, *7*, 717–726.
(6) (a) Koshkin, A. A.; Singh, S. K.; Nielsen, P.; Rajwanshi, V. K.; Kumar, R.; Meldgaard, M. C.; Olsen, E.; Wengel, J. *Tetrahedron* **1998**, *54*, 3607–3630. (b) Singh, S. K.; Nielsen, P.; Koshkin, A. A.; Wengel, J. *Chem. Commun.* **1998**, 455–456. (c) Kaur, H.; Babu, B. R.; Maiti, S. *Chem. Rev.* **2007**, *107*, 4672–4697. (d) Lebreton, J.; Escudier, J. M.; Arzel, L.; Len, C. *Chem. Rev.* **2010**, *110*, 3371–3418.
(7) Obika, S.; Nanbu, D.; Hari, Y.; Morio, K.; In, Y.; Ishida, T.; Imanishi, T *Tetrahedron Lett.* **1997**, *38*, 8735–8738.
(8) Petersen, M.; Bondensgaard, K.; Wengel, J.; Jacobsen, J. P. *J. Am. Chem. Soc.* **2002**, *124*, 5974–5982.
(9) Veedu, R. N.; Wengel, J. *Chem. Biodiversity* **2010**, *7*, 536–542.
(10) Swayze, E. E.; Siwkowski, A. M.; Wancewicz, E. V.; Migawa, M. T.; Wyrzykiewicz, T. K.; Hung, G.; Monia, B. P.; Bennett, C. F. *Nucleic Acids Res.* **2007**, *35*, 687–700.
(11) Morita, K.; Takagi, M.; Hasegawa, C.; Kaneko, M.; Tsutsumi, S.; Sone, J.; Ishikawa, T.; Imanishi, T.; Koizumi, M. *Bioorg. Med. Chem.* **2003**, *11*, 2211–2226.
(12) Zhou, C.; Chattopadhyaya, J. *Curr. Opin. Drug Discovery Dev.* **2009**, *12*, 876–898.
(13) Enderlin, G.; Nielsen, P. *J. Org. Chem.* **2008**, *73*, 6891–6894.
(14) Seth, P. P.; Vasquez, G.; Allerson, C. A.; Berdeja, A.; Gaus, H.; Kinberger, G. A.; Prakash, T. P.; Migawa, M. T.; Bhat, B.; Swayze, E. E. *J. Org. Chem.* **2010**, *75*, 1569–1581.
(15) Varghese, O. P.; Barman, J.; Pathmasiri, W.; Plashkevych, O.; Honcharenko, D.; Chattopadhyaya, J. *J. Am. Chem. Soc.* **2006**, *128*, 15173–15187.
(16) Hari, Y.; Obika, S.; Ohnishi, R.; Eguchi, K.; Osaki, T.; Ohishi, H.; Imanishi, T. *Bioorg. Med. Chem.* **2006**, *14*, 1029–1038.
(17) Abdur Rahman, S. M.; Seki, S.; Obika, S.; Yoshikawa, H.; Miyashita, K.; Imanishi, T. *J. Am. Chem. Soc.* **2008**, *130*, 4886–4896.
(18) Zhou, C.; Liu, Y.; Andaloussi, M.; Badgujar, N.; Plashkevych, O.; Chattopadhyaya, J. *J. Org. Chem.* **2009**, *74*, 118–134.
(19) Srivastava, P.; Barman, J.; Pathmasiri, W.; Plashkevych, O.; Wenska, M.; Chattopadhyaya, J. *J. Am. Chem. Soc.* **2007**, *129*, 8362–8379.
(20) Xu, J.; Liu, Y.; Dupouy, C.; Chattopadhyaya, J. *J. Org. Chem.* **2009**, *74*, 6534–6554.
(21) Zhou, C.; Plashkevych, O.; Chattopadhyaya, J. *Org. Biomol. Chem.* **2008**, *6*, 4627–4633.
(22) Albæk, N.; Petersen, M.; Nielsen, P. *J. Org. Chem.* **2006**, *71*, 7731–7740.
(23) Kumar, S.; Hansen, M. H.; Albæk, N.; Steffansen, S. I.; Petersen, M.; Nielsen, P. *J. Org. Chem.* **2009**, *74*, 6756–6769.

**SCHEME 1. Retrosynthetic Analysis to C8′-Modified Carba-ENA Thymidine**

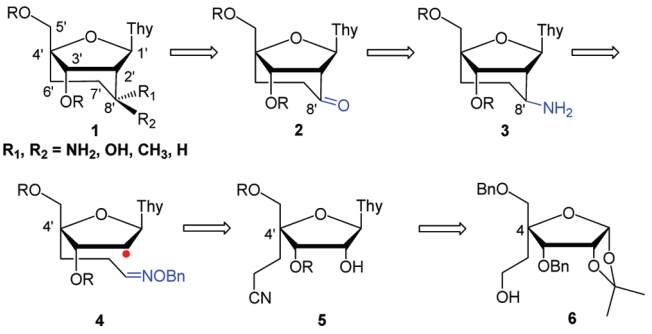


compared with those of AON with carba-ENA modification. On the basis of the results provided, we show how the nature and stereochemical orientation of C8′ substituents on carba-ENA modulate the biophysical and biological properties of modified AONs, which, in turn, we believe will enable us to design more promising nucleoside analogues as potential nucleic acids-based therapeutic or diagnostic reagents.

## Results and Discussion

**1. Synthesis of 8′-Modified-Carba-ENA Thymidine Analogues.** As shown in the retrosynthetic analysis in Scheme 1, the C8′-modified carba-ENA thymidine analogues can readily be accomplished exploiting cyclic ketone **2** that was synthesized from 8′-amino-carba-ENA thymidine **3**, which we obtained through free-radical cyclization of the oxime ether **4**. The oxime ether function can be introduced starting from nitrile **5**, which in turn can be easily obtained from known sugar precursor **6**[19] by a simple nucleophilic substituent with cyanide ion.[24]

**1.1. Synthesis of 8′-Amino-Carba-ENA Thymidine (15).** The synthetic route to 8′-amino-carba-ENA thymidine **15** and its phosphoramdite **18a**/**18b** is shown in Scheme 2. Treatment of the known sugar precursor **6**[19] with tosyl chloride, triethylamine, and DMAP in dichlormethane furnished tosylate **7**.[24] After workup, the crude tosylate was directly subjected to substitution with tetrabutylammonium cyanide (TBACN) in DMF to afford the desired 4-*C*-cyanoethyl-D-ribofuranose **8** in an overall yield of 77% from **6**.[25] Compound **8** was treated with a mixture of acetic acid, acetic anhydride, and triflic acid at 10 °C for 1 h to give diacetate **9** as an anomeric mixture. Glycosylation of the crude **9** provided exclusively $\beta$-configured thymine nucleoside **10** through a modified Vorbrüggen-type reaction in 85% yield in two steps.[15] Deacetylation of the 2′-*O*-acetyl group was achieved by treating compound **10** with 30% methylamine solution in ethanol at room temperature to furnish the desired product **11** in 94% yield. Then the nitrile group of **11** was reduced with diisobutylaluminum hydride (DIBALH) at −78 °C for 2 h to the corresponding aldehyde, which was subsequently subjected to oximation with *O*-benzylhydroxylamine to provide *O*-benzyl oxime **12** as a mixture of *E* and *Z* isomers in 61% yield.[26] After esterification of 2′-OH in nucleoside **12** with phenyl chlorothioformate in pyridine, the key precursor for radical cyclization, 2′-*O*-phenoxythiocarbonyl (PTC)-4′-*C*-(benzyloxyimino)propyl-thymidine **13**, was obtained in 88% yield. It has been reported that the configuration of the oximino-ether group does not affect the chemical yield or stereoselectivity of radical cyclization,[27] thus the *Z*/*E* mixture of **13** was directly subjected to radical cyclization, which was performed smoothly utilizing tributyltin hydride ($Bn_3SnH$) with AIBN as radical initiator in degassed toluene at $< 110$ °C, in order to avoid the decomposition of the starting material. To avoid the side reactions, starting material was highly diluted, and $Bn_3SnH$ and AIBN were added dropwise slowly (Experimental Section). As previously reported,[28,29] the radical reaction proceeded in the 6-*exo* cyclization mode to afford the sole product **14** in 60% yield. Meanwhile 1D NOE experiments proved that the configuration of C8′ was *R* stereochemistry. Subsequently, selective debenzylation of 8′-*N*-OBn was achieved with 10% Pd/C and ammonium formate as hydrogenolysis reagent at room temperature to produce the highly polar product **15** without any loss of 3′- and 5′-*O*-benzyl groups. The effort to protect 8′-amino with ethyl trifluoroacetate[20] was unsuccessful because of very low yield; merely about 20% even when 20 equiv of the reagent was added. Instead, the more reactive trifluoroacetic anhydride[30] was found to be a superior choice: Treatment of **15** with trifluoroacetic anhydride in pyridine and $CH_2Cl_2$ gave the expected compound **16a** in 60% yield. The structural integrity of the product was confirmed through $^{13}C$ NMR experiment, in which two typical quartet peaks around 110 and 150 ppm for the trifluoroacetyl group (TFA) were observed. Then **16a** was subjected to debenzylation involving 20% $Pd(OH)_2/C$ and cyclohexene as hydrogen donor at reflux and subsequent 5′-dimethoxytritylation to give the corresponding product **17a**. Unfortunately, significant loss of TFA during debenzylation has been observed, resulting in lower yield (30%) from **16a** to **17a**. To overcome this problem, the phenoxyacetyl group (PAC) was employed as a more stable protective group to afford **16b**,[31] which can be debenzylated completely under the same condition without any acylamino cleavage, followed by 5′-dimethoxytritylation to acquire **17b** in 72% yield. Phosphitylation of **17a** and **17b** with 2-cyanoethyl *N*,*N*-diisopropylphosphoramidochloridite was achieved to give the desired amidites **18a** and **18b** as a diastereomeric mixture in 93% and 70% yield, respectively.

**1.2. Synthesis of Carba-ENA-T 25, 8′-OH-Carba-ENA-T 22a/b, and 8′-Me-Carba-ENA-T 29 Starting from 8′-Amino-Carba-ENA-T 15.** Transformation of the 8′-amino to ketone (**15** → **19**) function was a key step for the synthesis of carba-ENA-T **25**, 8′-OH-carba-ENA-T **22a/b**, and 8′-Me-carba-ENA-T **29** starting from 8′-amino-carba-ENA-T **15** (Scheme 3). Oxidation of benzyloxyamine by MCPBA to oxime followed by treatment with Dess−Martin periodinane reagent has been shown in the previous study[20,32] to be an efficient strategy for

(24) Morita, K.; Takagi, M.; Hasegawa, C.; Kaneko, M.; Tsutsumi, S.; Sone, J.; Ishikawa, T.; Imanishi, T.; Koizumi, M. *Bioorg. Med. Chem.* **2003**, *11*, 2211–2226.
(25) Åkerfeldt, K. S.; Bartlett, P. A. *J. Org. Chem.* **1991**, *56*, 7133–7144.
(26) Kumar, V.; Gauniyal, M. H.; Shaw, K. A. *Tetrahedron: Asymmetry* **2007**, *18*, 2069–2078.
(27) Miyabe, H.; Torieda, M.; Inoue, K.; Tajiri, K.; Kiguchi, T.; Naito, T. *J. Org. Chem.* **1998**, *63*, 4397–4407.
(28) Marco-Contelles, J.; Martinez-Grau, A.; Martinez-Ripoll, M.; Cano, H.; Foces-Foces, C. *J. Org. Chem.* **1992**, *57*, 403–406.
(29) Marco-Contelles, J.; Pozuelo, C.; Jimeno, M. L.; Martinez, L.; Martinez-Grau, A. *J. Org. Chem.* **1992**, *57*, 2625–2631.
(30) Wenska, M.; Honcharenko, D.; Pathmasiri, W.; Chattopadhyaya, J. *Heterocycles* **2007**, *73*, 303–324.
(31) Honcharenko, D.; Varghese, O. P.; Plashkevych, O.; Barman, J.; Chattopadhyaya, J. *J. Org. Chem.* **2006**, *71*, 299–314.
(32) Simpkins, N. S.; Stokes, S.; Whittle, A. J. *J. Chem. Soc., Perkin Trans. I* **1992**, 2471–2477.

**SCHEME 2. Synthesis of 8′-Amino-Carba-ENA Thymidine**[a]

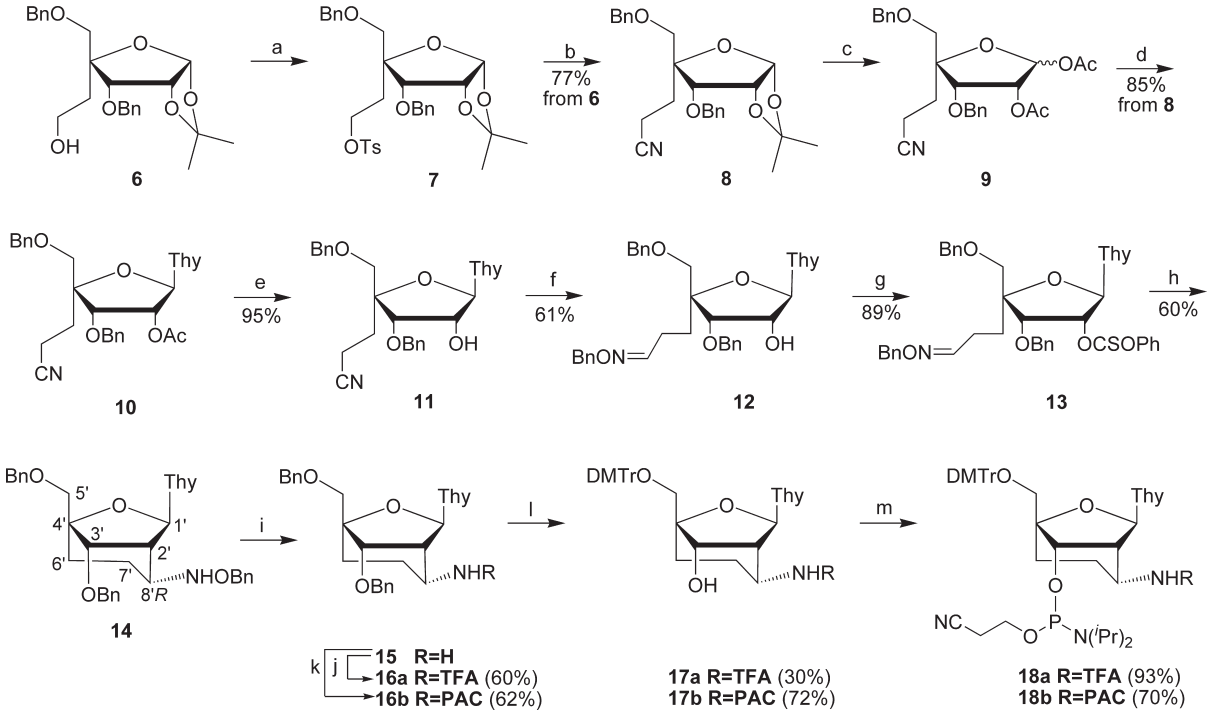


[a]Reagents and conditions: (a) tosyl chloride, $Et_3N$, DMAP, $CH_2Cl_2$, rt, overnight; (b) TBACN, DMF, rt−35 °C, 77% in two steps; (c) $Ac_2O$, AcOH, TfOH, 10 °C, 1 h; (d) thymine, BSA, TMSOTf, MeCN, reflux, overnight, 85% in two steps; (e) methylamine solution, methanol, 0 °C, 1 h, 95%; (f) 1 M DIBAL in toluene, $CH_2Cl_2$, −78 °C, 3 h; $BnONH_2 \cdot HCl$, pyridine, $CH_2Cl_2$, reflux, 1 h, 61% in two steps; (g) phenyl chlorothionoformate, pyridine, rt, 2 h, 89%; (h) $Bu_3SnH$, AIBN, toluene, 110 °C, 6 h, 60%; (i) 10% Pd/C, ammonium formate, methanol, rt, 8 h; (j) trifluoroacetic anhydride, pyridine, $CH_2Cl_2$, rt, 2 h, 60% (from **14**); (k) phenoxyacetyl chloride, pyridine, rt, overnight, 62% (from **14**); (l) 20% $Pd(OH)_2$/C, cyclohexene, ethanol, reflux, overnight; DMTr-Cl, pyridine, rt, overnight, 30% for **17a**, 72% for **17b**; (m) 2-cyanoethyl *N*,*N*-diisopropylphosphoramidochloridite, DIPEA, $CH_2Cl_2$, rt, 3 h, 93% for **18a**, 70% for **18b**.

this transformation, but in this case, oxidation of benzyloxyamine **14** by MCPBA only gave the corresponding oxime in 20% yield. Oxidative deamination[33] is another strategy for transformation of the second amino to ketone directly. Thus, different oxidative deamination reagents such as aqueous hypochlorite,[34] trichloroisocyanuric acid,[35] and copper−ascorbic acid dyad[36] have been tried but neither worked in our case. Instead, 3,5-di-*tert*-butyl-1,2-benzoquinone was found to be a satisfactory oxidative deamination reagent, and it efficaciously oxidized amine **15** to ketone **19** in an acceptable yield.[37] Reduction of **19** with $NaBH_4$ furnished two diastereomeric products **20a** (69%) and **20b** (19%). The major product **20a** has 8′*S* stereochemistry, suggesting that the hydride attack took place from the back of the carbocycle. Clearly, the hydride attack from the back is much more favored than the attack from the front of carbocycle, most likely owing to steric hindrance of the bulky 3′-*O*-benzyl group in the front face. After protection of free 8′-OH in **20a** and **20b** with the *p*-toluoyl group, the obtained compounds **21a** (90%) and **21b** (89%) were subjected to debenzylation followed by selective 5′-dimethoxytritylation to give **22a** (63%) and **22b** (83%), respectively, in satisfactory yields. Special care was taken for the debenzylation of **21a** because thermodynamically favored migration of the 8′-*O*-toluoyl group to the 3′-hydroxyl group in **21a** is possible owing to their *cis* orientation in a spatial proximity. Thus amount of hydrogenolysis reagent was increased (20% $Pd(OH)_2$/C, 1500 mg/mmol substrate and ammonium formate, 60 equiv) and reaction time was shortened for debenzylation of **21a**,[18] under which the benzyl groups were completely removed without cleavage and migration of the toluoyl group. Due to steric hindrance of the 8′-*O*-toluoyl group, 3′-*O*-phosphitylation of **22a** with 2-cyanoethyl *N*,*N*-diisopropylphosphoramidochloridite was allowed to proceed overnight to afford the resulting phosphoramidite **30a** in 71% yield, whereas the phosphitylation of **22b** under the same condition furnished phosphoramidite **30b** in 80% yield in only 3 h.

Starting from intermediate **20a**, parent carba-ENA-T **25** has been synthesized through radical deoxygenation of the 8′-OH in **20a** (Scheme 3). Considering the steric proximity between 3′-*O*-benzyl and 8′-hydroxyl groups in **20a**, the more reactive and smaller (methylthio)thiocarbonate was chosen as the radical-generating group.[38] Thus, **20a** was converted through the three-component reaction to radical precursor **23** (53%), which was subjected to the standard radical deoxygenation procedure[20] to give the expected parent carba-ENA thymidine **24** in 74% yield.

(33) (a) Neumann, R.; Levin, M. *J. Org. Chem.* **1991**, *56*, 5707–5710. (b) Barman, D. C.; Saikia, P.; Prajapati, D.; Sandhu, J. S. *Synth. Commun.* **2002**, *32*, 3407–3412. (c) Richey, H. G., Jr.; Erickson, W. F. *J. Org. Chem.* **1983**, *48*, 4349–4357.

(34) Lee, G. A.; Freedman, H. H. *Tetrahedron Lett.* **1976**, *20*, 1641–1644.

(35) Luca, L. D.; Giacomelli, G. *Synlett* **2004**, *12*, 2180–2184.

(36) Srogl, J.; Voltrova, S. *Org. Lett.* **2009**, *11*, 843–845.

(37) (a) Corey, E. J.; Achiwa, K. *J. Am. Chem. Soc.* **1969**, *91*, 1429–1432. (b) Klein, R. F. X.; Bargas, L. M.; Horak, V. *J. Org. Chem.* **1988**, *53*, 5994–5998.

(38) Mereyala, H. B.; Pola, P. *Synth. Commun.* **2002**, *32*, 2453–2458.

**SCHEME 3. Synthesis of Carba-ENA Thymidine (24) and Its Analouges**[a]

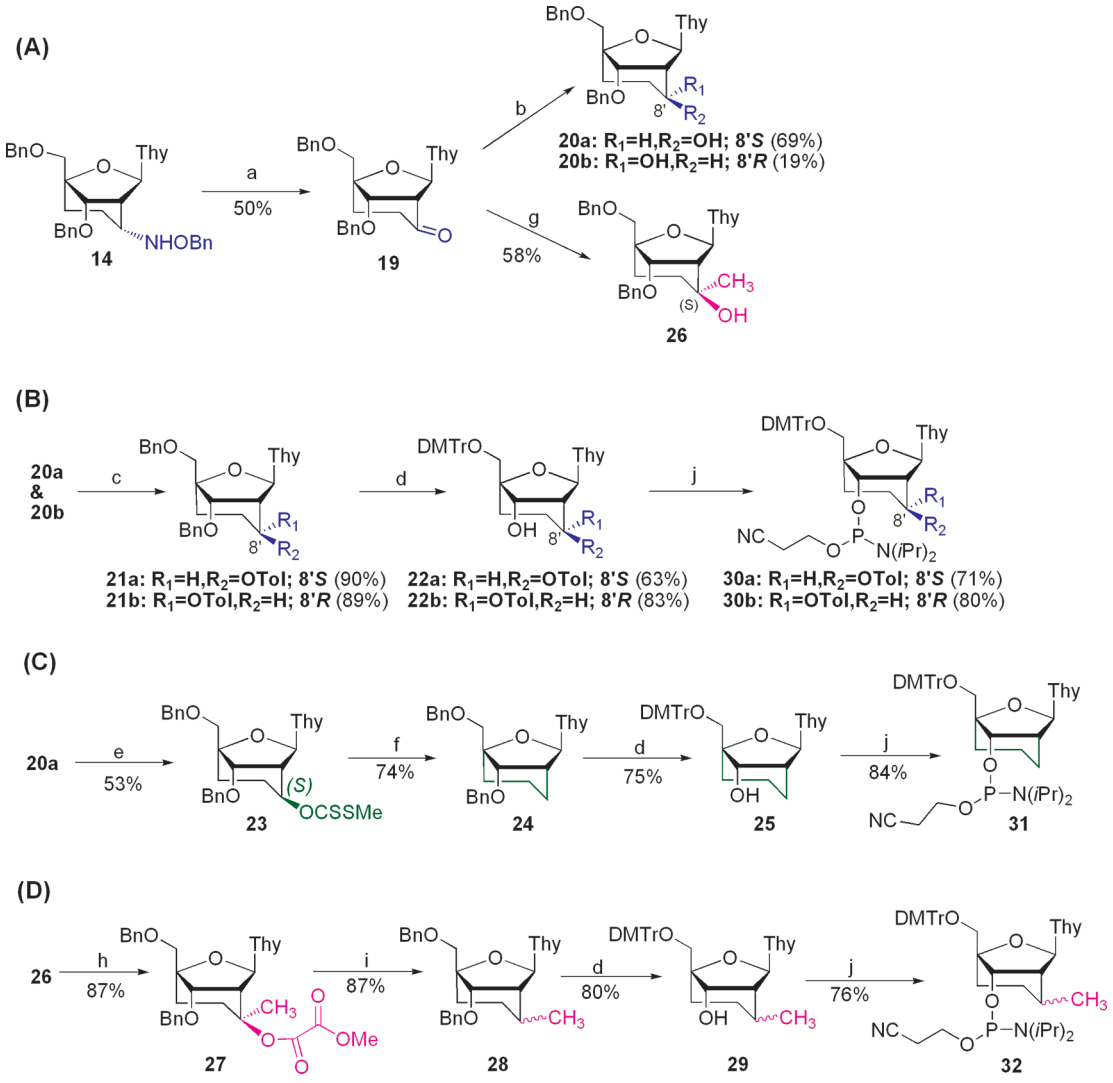


[a]Reagents and conditions: (a) (i) 10% Pd/C, ammonium formate, methanol, rt, 8 h; (ii) 3,5-di-*tert*-butyl-1,2-benzoquinone, methanol, THF, 40 °C,10 h; oxalic acid, $H_2O$, 40 °C, overnight, 50% in two steps; (b) $NaBH_4$, ethanol, rt, 4 h, 69% for **20a** and 19% for **20b**; (c) *p*-toluoyl chloride, pyridine, rt, overnight, 90% for **21a**, 89% for **21b**; (d) 20% $Pd(OH)_2$/C, ammonium formate, methanol, reflux; DMTr-Cl, pyridine, rt, overnight, 63% for **22a**, 83% for **22b**, 75% for **25**, 80% for **29**; (e) NaH, $CS_2$, MeI, THF, 40 °C−rt, 53% (from **20a**); (f) $Bu_3SnH$, AIBN, toluene, reflux, 1.5 h, 74%; (g) 1.6 M MeLi in $Et_2O$, THF, −78 °C, 10 h, 58%; (h) methyl oxalyl chloride, pyridine, 40 °C, overnight, 87%; (i) $Bu_3SnH$, AIBN, toluene, reflux, 4 h, 87%; (j) 2-cyanoethyl *N*,*N*-diisopropylphosphoramidochloridite, DIPEA, $CH_2Cl_2$, rt, 71% for **30a**, 80% for **30b**, 84% for **31**, 76% for **32**.

Finally, carba-ENA-T with a hydrophobic C8′ substituent, 8′-Me-carba-ENA-T **29**, has been synthesized starting from key intermediate ketone **19** by a known strategy.[18] Instead of methyl magnesium iodide,[39] treatment of ketone **19** with methyl lithium in THF for 8 h furnished the sole product **26** (58%),[40] in which the 8′*S*-configuration was confirmed by 1D NOE experiment. Hence, the methyl anion attacked the ketone exclusively from the back of the carbocycle, which is consistent with the stereoselective reduction on ketone **19** by $NaBH_4$. To remove the 8′-hydroxyl group, intermediate **26** reacted with methyl(chlorocarbonyl)-formate in pyridine at 40 °C to give **27** in 87% yield,[41] which was subjected to a standard radical deoxygenation to give two inseparable diastereomers **28** (8′*S*:8′*R* = 5:4) in 87% yield. Relative lack of stereoselectivity during the free-radical reaction is likely to be due to higher reaction temperature. To provide appropriately protected building blocks for standard automated solid-phase oligonucleotide synthesis by using the phosphoramidite approach, nucleosides **24** and **28** were debenzylated followed by 5′-*O*-dimethoxytritylation to give **25** and **29** in 75% and 80% yield, respectively. Subsequently, the resulting compounds **25** and **29** were converted into the respective 3′-*O*-phosphoramidites **31** (84%) and **32** (76%) under standard condition.

**1.3. NMR Characterization of Key Intermediates Involved in the Synthesis of the 8′-Functionalized Carba-ENA Thymidines.** Structures of all intermediates and final products were confirmed by $^1H$, $^{13}C$, COSY, $^1H-^{13}C$ HMQC and HMBC

(39) Kakefuda, A.; Yoshimura, Y.; Sasaki, T.; Matsuda, A. *Tetrahedron* **1993**, *49*, 8513–8528.
(40) Matsuda, A.; Itoh, H.; Takenuki, K.; Sasaki, T.; Ueda, T. *Chem. Pharm. Bull.* **1988**, *36*, 945–953.
(41) (a) Dolan, S. C.; Macmillian, J. *J. Chem. Soc., Chem. Commun.* **1985**, 1588–1589. (b) Pettit, G. R.; Melody, N.; Herald, D. L.; Knight, J. C.; Chapuis, J. *J. Nat. Prod.* **2007**, *70*, 417–422.

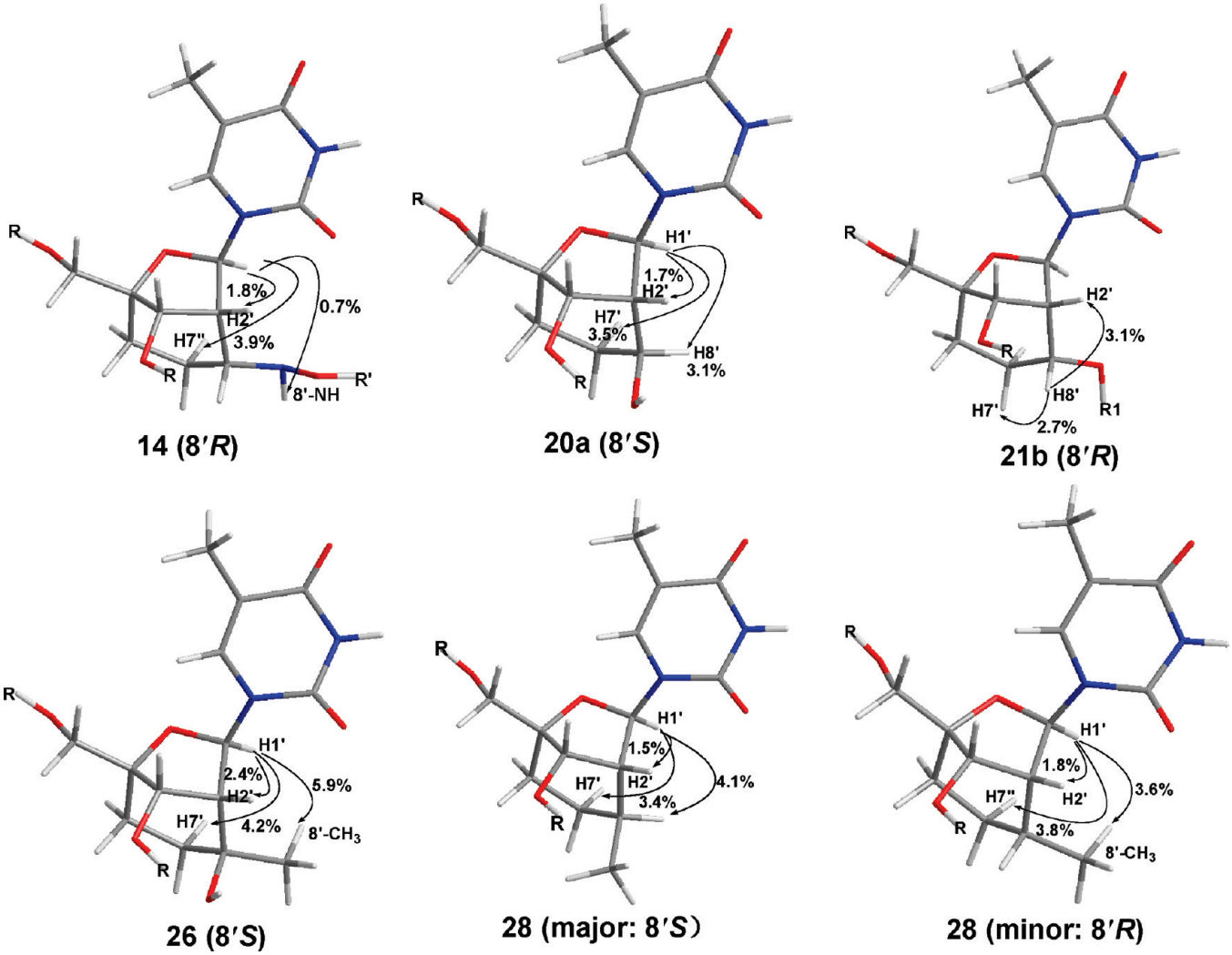


**FIGURE 1.** The NOE contacts of the key intermediates (**14**, **20a**, **21b**, **26**, and **28**). R = Bn, $R_1$ = Tol.

NMR, and mass spectroscopy (see the Supporting Information). The $^1$H NMR spectra of all carba-ENA derivatives showed a singlet for H1′ as found for all 2′,4′-fused bicyclic nucleosides, which strongly suggested the North-type sugar pucker.[42]

For compound **14**, the correlation between H2′ with H8′ in COSY NMR spectra gave evidence to the bicyclic system formed during the free-radical cyclization, which is further consolidated by the observation of the long-range correlations between H2′ with C7′ and between H1′ with C8′ in HMBC NMR spectra. In the 1D NOE experiment, irradiation of H1′ led to NOE enhancement for 8′-NH (0.7%), H2′ (1.8%), and H7″ (3.9%), but none for H8′ (Figure 1), which identified C8′ in the 8′*R*-configuration.

The orientation of C8′ substituents in intermediates **20a**, **20b**, **26**, and **28** has been assigned by 1D NOE experiments. In compound **20a**, the strong enhancement for H8′ (3.1%) and H7′ (3.5%) was observed upon irradiation of H1′, confirming the *S*-configuration for C8′. Severe overlap of signals of H8′ and H3′ in compound **20b** made it hard to determine the configuration of C8′ by 1D NOE experiments at this stage. The configuration of C8′ in **20b**, however, could be assigned to the *R*-configuration since compound **21b** has been found to have the C8′ *R*-configuration: irradiation of H8′ in **21b** resulted in the enhancement for H2′ (3.1%) and H7′ (2.7%), but not for H1′. For compound **26**, the strong NOE enhancement for the 8′-methyl group (5.9%) and H7′ (4.2%) upon irradiation of H1′ clearly indicated the *S*-configuration for C8′. By comparing the observation that irradiation on H1′ in the major product of **28** caused remarkable enhancement for H8′ (4.1%) and none for 8′-Me, in contradistinction to the minor product of **28**, which led to notable NOE enhancement for 8′-Me (3.6%) but none for H8′, it was concluded that the C8′ is *S* in the major product, whereas *R* in the minor product.

On the other hand, the coupling constants also have been used to identify the configuration of chiral center in these derivatives. The six-membered carbocyclic ring of carba-ENA adopts a typical chair conformation.[18,22] Through decoupling experiments, the observation of a small coupling constant (~6 Hz) between H8′ and axial H7′ and a large one (~11 Hz) between H8′ and equatorial H7″ in **16b** and **21b** implied H8′ and equatorial H7′ have torsion angles in gauche but that of H8′ and axial H7″ in trans, according with the 8′*R*-configuration. On the contrary, the $^3J_{H7''H8'}$ in **17a** is 0 Hz,

(42) Obika, S.; Nanbu, D.; Hari, Y.; Morio, K.; In, Y.; Ishida, V. K.; Sing, S. K.; Wengel, J. *J. Am. Chem. Soc.* **1998**, *120*, 13252–13253.

**SCHEME 4. Mechanism of Radical Cyclization Reaction**

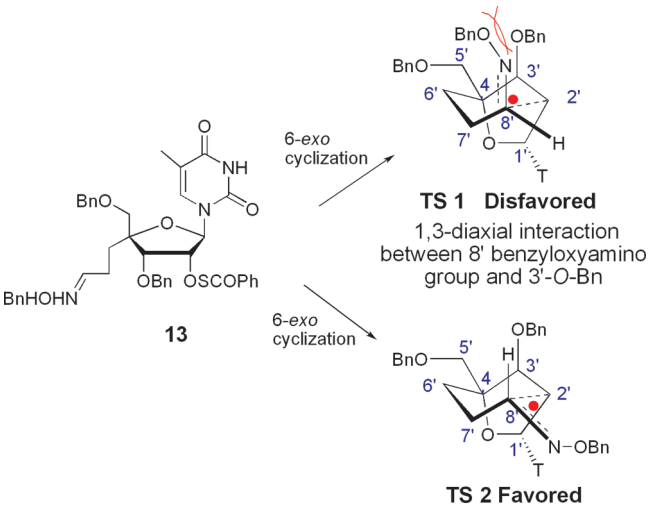


which suggested the H8′ and axial H7′′ is nearly 90°, Hence C8′ has an *S* stereochemistry (Figures SII 8−13, Supporting Information). The results obtained from decoupling experiments conformed to those from 1D NOE experiments.

**1.4. Mechanism of the Ring-Closure Reaction.** During radical mediated 6-*exo* cyclization of compound **13**, the in situ generated C2′ carbon radical could attack the oxime intramolecularly through both faces of C=N, forming two possible transition states TS1 and TS2 (Scheme 4). 1,3-Diaxial disposition between the forming bulky benzyloxyamino substituent and 3′-*O*-benzyl group in TS 1 is energetically disfavored. In contrast, the benzyloxyamino group in TS 2 points equatorially, leading to minimal steric repulsion between C8′ and C3′ substituents. As a result, compound **14** that has *R* stereochemistry at chiral C8′ has been observed as the exclusive product.

**2. Synthesis and Purification of Oligonucleotides Containing 8′-Modified Carba-ENA Thymidine Analogues.** Through solid-phase DNA synthesis protocol[43] on an automated DNA/RNA synthesizer, the phosphoramidites **18b**, **30a**/**b**, **31**, and **32** were incorporated as monosubstitution into a 15mer DNA sequence as used in our former studies.[18,20] The coupling time of building blocks **18b**, **30b**, **31**, and **32** was about 10 min, whereas for **30a** the coupling time was prolonged to 15 min, in view of steric obstruction by the 8′-*O*-toluoyl group during the coupling. The satisfactory coupling yields (40−75%) were obtained for all compounds. The sequences, modification site, and structure of modification are shown in Table 1. For AONs **2**−**9** the treatment with 33% aqueous ammonia at room temperature overnight was carried out to cleave oligos from the solid support as well as for the removal of the protecting groups. On the other hand, considering the stability of PAC and Tol groups, the solid support for AONs **10**−**17** and **18**−**21** was incubated in aqueous ammonia at 55 °C for 1 to 3 days. Unfortunately, the PAC groups in AONs **18**−**21** are too stable to be removed. A stronger deprotection reagent such as 1 N NaOH solution, however, led to degradation of oligonucleotides.[44,45] Thus, building block **18a** with a trifluoroacetyl-protecting group was used to synthesize AONs **22**−**25** following the standard procedure. Meanwhile, ENA-T phosphoramidite was synthesized according to a reported procedure[11] (see the Supporting Information), and was incorporated into AONs **30**−**33** for comparison. The fully deprotected AONs were purified by 20% denatured PAGE and their structural integrity was confirmed by MALDI-TOF mass measurement (Table SII 1, Supporting Information).

**3. Hybridization Studies of Carba-ENA Analogues-Modified AONs with Complementary RNA and DNA.** The hybridization properties of the modified oligonucleotides toward complementary DNA and RNA were studied by thermal denaturation experiments. The melting temperature ($T_m$) values of duplex formed by AONs **2**−**33** with the complementary DNA or RNA were measured, and their $\Delta T_m$ values provided by comparing with the native AON **1** were listed in Table 1. The $\Delta T_m$ values of AON **26**−**29** that have been reported previously[18] are also listed in Table 1 for comparison.

**3.1. Comparison of Carba-ENA (Type I) Modification with Native Counterpart and ENA (Type VIII) Modification.** Albæk et al. reported that the $\Delta T_m$ value of duplexes formed by parent carba-ENA-U with complementary RNA was +4.5 °C,[22] whereas our present result showed that one parent carba-ENA-T modification in AON:RNA duplex resulted in an increase of 1.4 °C in $T_m$. The notable disparity between the exact $\Delta T_m$ value obtained by us and those by Albæk et al. is likely due to the sequence difference.

One ENA (type VIII) modification in the AON strand resulted in a $T_m$ increase of 3.6 °C for the AON:RNA duplex, which is a much higher stabilization effect than the parent carba-ENA modification (+1.4 °C/modification). We have previously reported[20] that in the same AON sequence, LNA modification (+4.5 °C/modification) also led to much higher $T_m$ increase for the AON:RNA duplex than the parent carba-LNA modification (+3.6 °C/modification). Hence, it seems that the 2′-oxygen on the bicyclic system plays an important role in the thermal stability of the AON:RNA duplex. One of the plausible explanations for the role of 2′-oxygen could be that the 2′-oxygen is engaged in the hydrogen bonding to water molecules, whereas it is well-known[46] the extensive hydration network in the minor groove can reduce the electrostatic repulsion of the internucleotidic phosphates, thus stabilizing the AON:RNA duplex. Although this 2′-oxygen in LNA or ENA incorporated oligos has a $T_m$ increase effect with complementary RNA, it, however, reduces the nucleolytic stability considerably compared to their carbocyclic counterparts (see section 4).

**3.2. Comparison of Type IV, Type VI, and Type VII with Type I Modifications.** One [8′*R*-OH]-carba-ENA (type IV), [8′*R*-Me]-carba-ENA (type VII), and [8′*R*-$NH_2$]-carba-ENA (type VI) modification in AON leads to $T_m$ increase for the AON:RNA duplex around 0.6, 0.5, and 0.8 °C, respectively (Table 1), which are slightly lower than the effect imposed by the parent carba-ENA (type I) modification (+1.4 °C/modification). This observation indicates the C8′ substituents, regardless of hydrophilic hydroxyl and amino group or hydrophobic methyl group, destabilize the AON:RNA duplexes slightly when they face away from the vicinal 3′-phosphate.

(43) Beaucage, S. L.; Caruthers, M. H. *Current Protocols in Nucleic Acid Chemistry*; John Wiley & Sons: New York, 2003.
(44) Ditrich, K.; Ladner, W.; Melder, J. US Patent US6713652 B1, 2000.
(45) Heinz, L. J.; Lunn, W. H. W.; Schoepp, D. D. Patent EP658539, 1995.
(46) Tereshko, V; Gryaznov, S.; Egli, M. *J. Am. Chem. Soc.* **1998**, *120*, 269–283.

**TABLE 1. Thermal Denaturation of Duplexes of Native and Carba-ENA Analogues-Modified AONs with Complementary DNA or RNA[a]**

| Entry | Modified Carba-ENA Structures: **Types I-VIII** | AON-Sequence[a] *[Encompassing modifications in the minor groove]* | With DNA $T_m$ (°C) | Minor groove Average $\Delta T_m$(aver)[b] in AON:DNA | With RNA $T_m$ (°C) | Minor groove Average $\Delta T_m$(aver)[b] in. AON:RNA | RNA target selectivity $\Delta\Delta T_m$[c] |
|---|---|---|---|---|---|---|---|
| **AON1** | Native | 5'-d (CTT CAT TTT TTC TTC) | 45.0 | | 44.5 | | -0.5 |
| **AON2** | **Type I** 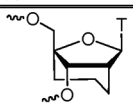 | 5'-d (CTT CAT TTT TTC *T*TC) | 44.5 | **-3.1** | 45.9 | **+1.4** | +1.4 |
| **AON3** | | 5'-d (CTT CAT TTT *T*TC TTC) | 41.5 | | 45.9 | | +4.4 |
| **AON4** | | 5'-d (CTT CAT T*T*T TTC TTC) | 40.7 | | 45.8 | | +5.1 |
| **AON5** | | 5'-d (CTT CA*T* TTT TTC TTC) | 40.8 | | 46.3 | | +5.5 |
| **AON6** | **Type II** 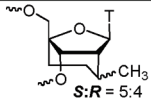 | 5'-d (CTT CAT TTT TTC *T*TC) | 42.6 | **-5.1** | 44.5 | **+0.3** | +1.9 |
| **AON7** | | 5'-d (CTT CAT TTT *T*TC TTC) | 39.0 | | 44.3 | | +5.3 |
| **AON8** | | 5'-d (CTT CAT T*T*T TTC TTC) | 38.8 | | 45.0 | | +6.2 |
| **AON9** | | 5'-d (CTT CA*T* TTT TTC TTC) | 38.9 | | 45.8 | | +6.9 |
| **AON10** | **Type III** 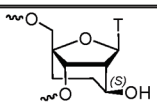 | 5'-d (CTT CAT TTT TTC *T*TC) | 42.6 | **-4.7** | 44.3 | **0** | +1.7 |
| **AON11** | | 5'-d (CTT CAT TTT *T*TC TTC) | 40.1 | | 44.7 | | +4.6 |
| **AON12** | | 5'-d (CTT CAT T*T*T TTC TTC) | 39.1 | | 44.5 | | +5.4 |
| **AON13** | | 5'-d (CTT CA*T* TTT TTC TTC) | 39.2 | | 45.0 | | +5.8 |
| **AON14** | **Type IV** 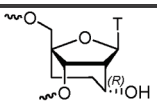 | 5'-d (CTT CAT TTT TTC *T*TC) | 43.1 | **-4.5** | 45.3 | **+0.6** | +2.2 |
| **AON15** | | 5'-d (CTT CAT TTT *T*TC TTC) | 39.7 | | 45.1 | | +5.4 |
| **AON16** | | 5'-d (CTT CAT T*T*T TTC TTC) | 38.7 | | 44.9 | | +6.2 |
| **AON17** | | 5'-d (CTT CA*T* TTT TTC TTC) | 40.1 | | 45.6 | | +5.5 |
| **AON18** | **Type V** 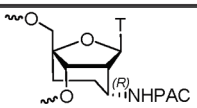 | 5'-d (CTT CAT TTT TTC *T*TC) | 44.9 | **-2.2** | 45.8 | **+1.2** | +0.9 |
| **AON19** | | 5'-d (CTT CAT TTT *T*TC TTC) | 41.7 | | 45.2 | | +3.5 |
| **AON20** | | 5'-d (CTT CAT T*T*T TTC TTC) | 41.6 | | 45.4 | | +3.8 |
| **AON21** | | 5'-d (CTT CA*T* TTT TTC TTC) | 42.8 | | 46.7 | | +3.9 |
| **AON22** | **Type VI** 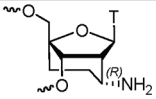 | 5'-d (CTT CAT TTT TTC *T*TC) | 44.8 | **-1.3** | 45.1 | **+0.8** | +0.3 |
| **AON23** | | 5'-d (CTT CAT TTT *T*TC TTC) | 43.9 | | 45.2 | | +1.3 |
| **AON24** | | 5'-d (CTT CAT T*T*T TTC TTC) | 42.7 | | 45.2 | | +2.5 |
| **AON25** | | 5'-d (CTT CA*T* TTT TTC TTC) | 43.1 | | 46.2 | | +3.1 |
| **AON26** | **Type VII[d]** 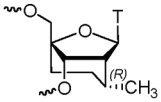 | 5'-d (CTT CAT TTT TTC *T*TC) | 44.0 | **-4.5** | 45.5 | **+0.5** | +1.5 |
| **AON27** | | 5'-d (CTT CAT TTT *T*TC TTC) | 40.0 | | 45.0 | | +5.0 |
| **AON28** | | 5'-d (CTT CAT T*T*T TTC TTC) | 40.0 | | 45.0 | | +5.0 |
| **AON29** | | 5'-d (CTT CA*T* TTT TTC TTC) | 40.0 | | 45.5 | | +5.5 |
| **AON30** | **Type VIII (ENA)[11]** 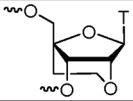 | 5'-d (CTT CAT TTT TTC *T*TC) | 46.4 | **-0.4** | 48.4 | **+3.6** | +2.0 |
| **AON31** | | 5'-d (CTT CAT TTT *T*TC TTC) | 44.3 | | 47.8 | | +3.5 |
| **AON32** | | 5'-d (CTT CAT T*T*T TTC TTC) | 43.3 | | 47.9 | | +4.6 |
| **AON33** | | 5'-d (CTT CA*T* TTT TTC TTC) | 44.2 | | 48.1 | | +3.9 |

[a]A = native 9-adeninyl, C = 1-cytosinyl, T = 1-thyminyl, "***T***" (shown in red) indicates the incorporated modified thymidine monomer with the specified structure shown in the table. Molecular weights of all antisense sequences are conformed by MALDI-TOF (see Table SII 1, Supporting Information). $T_m$ values measured as the maximum of the first derivative of the melting curve ($A_{260}$ nm vs temperature) in medium salt buffer (60 mM tris-HCl at pH 7.5, 60 mM KCl, 0.8 mM $MgCl_2$) with temperature range 20 to 70 °C, using 1 $\mu$M concentrations of two complementary strands. The value of $T_m$ given is the average of two or three independent measurements (the error of the three consecutive measurements is within ±0.3 °C). [b]$\Delta T_m$ values were obtained by comparing the $T_m$ values of modified AONs **2**−**33** with that of the native AON **1**. The $\Delta T_m$(aver) value obtained here is the average value from four AONs incorporated with the same compound at four different modification sites. [c]$\Delta\Delta T_m$ = ($T_m$ of AON:RNA) − ($T_m$ of AON:DNA). [d]Modifications of type VII have been taken from reported work,[18] and are used for $T_m$ comparison with our present series of modified AONs.

The less destabilizing effect of the 8′*R*-amino group than that of the 8′*R*-methyl or the hydroxyl group is presumably because in experimental buffer the amino group is partially protonated, and can reduce charge repulsion between phosphates on opposition strands through partial charge neutralization, which is a favorable contribution to the free energy of duplex formation.[47,48]

**3.3. Comparison of Type III with Type IV Modification.** [8′*S*-OH]-carba-ENA (type III) modification did not result in any $T_m$ change for the AON:RNA duplex, which is contrary to the observation that one [8′*R*-OH]-carba-ENA (type IV) modification led to a 0.6 °C increase in $T_m$. Hence, when the 8′-OH group points toward the vicinal 3′-phosphate, it renders a more negative effect for target RNA affinity than when it points away from the neighboring 3′-phosphate.

**3.4. Comparison of Type II with Type VII Modification.** It seems the orientation of hydrophobic 8′-Me exerts little if any effect on thermal stability of the AON:RNA duplex since we found type II ([8′-56%*S*/44%*R*-Me]-carba-ENA) and type VII ([8′*R*-Me]-carba-ENA) modification lead to very similar $T_m$ increase, 0.5 and 0.3 °C/modification, respectively.

**3.5. Comparison of Type V with Type VI Modification.** To investigate the influence of larger hydrophobic substituent in the minor groove of the AON:RNA duplex on the thermodynamic stability, the $T_m$ of duplexes formed by [8′*R*-NHPAC]-carba-ENA (type V)-modified AONs **18**−**21** with complementary RNA has also been measured. It was found that [8′*R*-NHPAC]-carba-ENA (type V) modification renders a

(47) Cuenoud, B.; Casset, F.; Hüsken, D.; Natt, F.; Wolf, R. M.; Altmann, K. H.; Martin, P.; Moser, H. E. *Angew. Chem., Int. Ed.* **1998**, *37*, 1288–1291.

(48) Prakash, T. P.; Püschi, A.; Lesnik, E.; Mohan, V.; Tereshko, V.; Egli, M.; Manoharan, M. *Org. Lett.* **2004**, *6*, 1971–1974.

relatively higher $T_m$ increase than [8′*R*-$NH_2$]-carba-ENA (type VI) modification (Table 1). This is an unusual observation, since the phenyl of PAC in type V modification is expected to perturb the hydration network in the minor groove, which we expected to result in a destabilization effect. One likely explanation for this unusual observation is that the phenyl group may intercalate into the hybrid duplex.

**3.6. The Carba-ENA-Modified AONs Are Highly RNA-Selective. a. Comparison of Carba-ENAs with Native.** Unlike in AON:RNA duplex, carba-ENAs modification in AON:DNA led to significant $T_m$ decrease compared to the native counterpart. Hence, carba-ENAs-modified AONs are more RNA-selective than the native. The RNA selectivity of carba-ENAs could be due to the fact that the DNA:DNA duplex has a narrower minor groove (ca. 5−6 Å) than the DNA:RNA hybrid (ca. 9−10 Å).[49] Hence, the carbocycle of carba-ENA, which is located at the minor groove, may cause more serious perturbation in AON:DNA than in the AON:RNA duplex. As a result, the $T_m$ value of the carba-ENA-modified AON:DNA homoduplex was pronouncedly decreased compared to that of the carba-ENA-modified AON:RNA heteroduplex.

**b. Comparison of Carba-ENAs with ENA.** The magnitude of RNA selectivity [denoted by $\Delta\Delta T_m$, $\Delta\Delta T_m$ = ($T_m$ of AON:RNA duplex) − ($T_m$ of AON:DNA duplex)] of carba-ENA modifications (types I, II, III, IV, and VII) is around 5−6 °C/modification (Table 1), which is significantly higher than that of ENA modification ($\Delta\Delta T_m$ = ∼3.5 °C/modification). By analyzing the $T_m$ data, we found the higher RNA selectivity of carba-ENA compared to ENA is because the carba-ENA modifications result in much more significant $T_m$ decrease for AON:DNA than the ENA modification (Table 1). Hence, it seems 2′-oxygen is more important for the thermal stability of the AON:DNA duplex than for the AON:RNA duplex.

**c. Comparison of Parent Carba-ENA with Parent Carba-LNA and LNA.** It has been reported previously by us[20] that parent carba-LNA-modified AON (around 5 °C/modification) are also more RNA selective than LNA-modified counterpart (3−4 °C/modification). Hence, it seems the relative RNA selectivity of parent carba-ENA, parent carba-LNA, ENA, and LNA follows this rank: parent carba-ENA ≈ parent carba-LNA > ENA ≈ LNA.

**4. Engineering the 3′-Exonuclease Stability in the Carba-ENA Analogues-Modified AONs.** It is known that 3′-exonuclease SVPDE-mediated phosphate scission involves recognition of the 3′-end nucleotide, followed by the attack by threonine residue of the enzyme on the phosphate in line with the 3′-*O* of the penultimate nucleotide, which subsequently departs.[50,51] The incorporation of modified nucleotides in AONs may regulate the enzymatic resistance of the vicinal phosphate. Here AONs **2**, **6**, **10**, **14**, **18**, **22**, and **30** with different modifications at position ***T***13 (position 3 from 3′-end, see Figure SII 14 in the Supporting Information) were adopted to test how these modifications influence the 3′-exonuclease resistance of the modified AONs. These AONs ($^{32}$P-labeled at 5′-end) were incubated with phosphodiesterase I from *Crotalus adamanteus venom* (SVPDE) [SVPDE 6.7 ng/μL, AON 3 μM, 100 mM Tris-HCl (pH 8.0), 15 mM $MgCl_2$, total reaction volume was 30 μL] at 21 °C. Aliquots were taken out at appropriate time intervals and analyzed by 20% denaturing PAGE. The gel pictures obtained upon autoradiography are shown in Figure SII 14 (Supporting Information). The [8′*R*-$CH_3$]-carba-ENA-modified AON **26**, [6′*R*-$CH_3$,8′*R*-$CH_3$]-carba-ENA-modified AON **34**, and [6′*S*-$CH_3$,8′*R*-$CH_3$]-carba-ENA-modified AON **35** that have been reported previously[18] were also treated with SVPDE in parallel for comparison purpose.

The native DNA (AON **1**) did not display any 3′-exonuclease resistance and was completely degraded within ∼4 min, whereas under the identical condition, all modified AONs exhibit improved exonuclease resistance to variable extents. Due to modified nucleotides locating at position ***T***13, the stability of both phosphate *P*14 and *P*13 (see Figure SII 14 in the Supporting Information for phopshate (*P*) numbering) has been remarkably improved toward 3′-exonuclease, so two bands corresponding to 14mer and 13mer on PAGE pictures can be observed. However, once the phosphate *P*13 is cleaved, AON could be degraded to the monomer blocks very rapidly.

**4.1. Relative Nuclease Resistance of Carba-ENA, ENA-Modified AONs.** Total percentages of integrated 14mer and 13mer AONs were plotted against time points to give SVPDE digestion curves (Figure 2) for each AON, and pseudo-first-order reaction rates were observed by fitting the curves to single-exponential decay functions. The stability of these AONs toward SVDPE incubation increases in the following sequences: AON **1** ≪ ENA-modified AON **30** ($k$ = 1.7704 ± 0.0812 $h^{-1}$) < [8′*R*-NHPAC]-carba-ENA-modified AON **18** ($k$ = 0.6761 ± 0.0386 $h^{-1}$) ≈ [8′*S*-OH]-carba-ENA-modified AON **10** ($k$ = 0.5131 ± 0.0530 $h^{-1}$) < [8′*R*-$NH_2$]-carba-ENA-modified AON **22** ($k$ = 0.3086 ± 0.0085 $h^{-1}$) < [8′*R*-Me]-carba-ENA-modified AON **26** ($k$ = 0.1249 ± 0.0042 $h^{-1}$) ≈ [8′*R*-OH]-carba-ENA-modified AON **14** ($k$ = 0.0985 ± 0.0027 $h^{-1}$) ≈ [8′*R*/*S*-Me]-carba-ENA-modified AON **6** ($k$ = 0.0881 ± 0.0034 $h^{-1}$) ≈ carba-ENA-modified AON **2** ($k$ = 0.0827 ± 0.0017 $h^{-1}$) < [6′*S*-Me-8′*R*-Me]-carba-ENA-modified AON **35** ($k$ = 0.0494 ± 0.0019 $h^{-1}$) ≈ [6′*R*-Me-8′*R*-Me]-carba-ENA-modified AON **34** (k = 0.0401 ± 0.0030 $h^{-1}$).

The above comparison leads us to the following conclusions:

**a. Replacement of 2′-Oxygen of ENA and LNA with the −$CH_2$− Group Significantly Increases the Nuclease Resistance.** Parent carba-ENA-T (type I)-modified AON **2** was about 20 times more stable than ENA-T-modified AON **30**. In our previous study, parent carba-LNA-T-modified AON has also been found to be about 50 times nucleolytically more stable than the LNA-T-modified counterpart. These observations highlighted the unique effect of replacement of 2′-oxygen with the *−$CH_2$− group* in improving the nuclease resistance of vicinal phosphates.

**b. 8′*R*-OH and 8′-Me Subsituents on Carba-ENA Only Have a Marginal Effect on the Nuclease Resistance.** This conclusion can be confirmed by the fact that AON **6**, **14**, and **26** showed very similar stability as parent carba-LNA-T-modified AON **2** (Figure 2).

**c. 8′*R*-$NH_2$ Substituent on Carba-ENA Significantly Decreases the Stability.** [8′*R*-$NH_2$]-carba-ENA-modified AON **22** is around four times less stable than parent carba-LNA-T-modified AON **2**. Moreover, [8′*R*-NHPAC]-carba-ENA-modified AON **18** was found to be even less stable then AON **22**.

**d. 8′*S* Substituent Can Render Totally Different Effect on the Nuclease Resistance Depending upon the Nature of the**

(49) Gyi, J. I.; Lane, A. N.; Conn, G. L.; Brown, T. *Biochemistry* **1998**, *37*, 73–80.
(50) Culp, J. S.; Butler, L. G. *Arch. Biochem. Biophys.* **1986**, *246*, 245–249.
(51) Cleland, W. W.; Hengge, A. C. *Chem. Rev.* **2006**, *106*, 3252–3278.

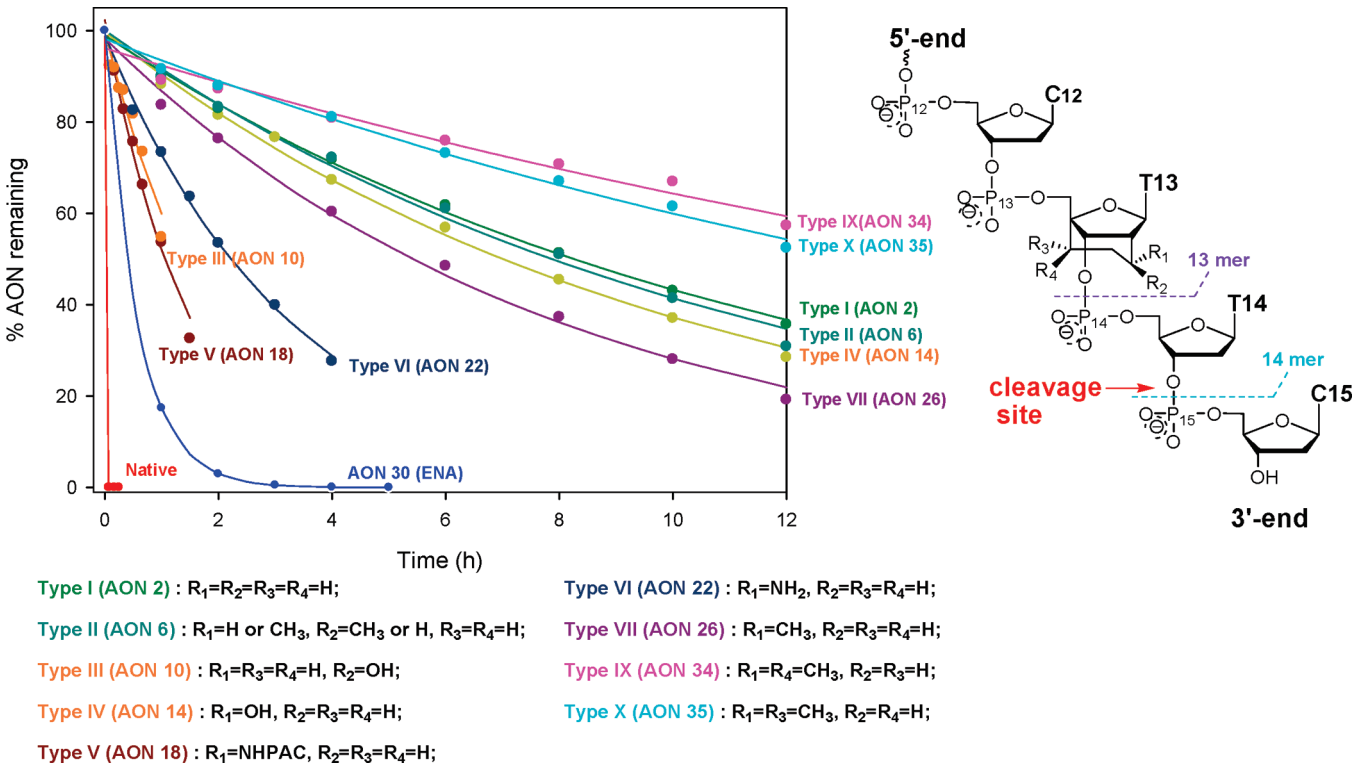


**FIGURE 2.** Amount of remaining initial oligonucleotide (taken 14mer and 13mer together in the calculation of % remaining) during 3′-exonuclease (SVPDE)-promoted digestion. Digestion condition: AON 3 $\mu$M (5′-end $^{32}$P labeled with specific activity 80 000 cpm), 100 mM Tris-HCl (pH 8.0), 15 mM $MgCl_2$, SVPDE 6.7 ng/$\mu$L, reaction temperature 21 °C, total reaction volume was 30 $\mu$L. Molecular structure of T13 modified AON with carba-ENA analogues was also shown in the figure.

**Substituent.** 8′*S*-OH substituent obviously destabilizes vicinal phosphate toward 3′-exonuclease given the faster degradation of [8′*S*-OH]-carba-ENA-modified AON **10**, but 8′*S*-Me substituent leads to a stabilization effect because [8′*R*/*S*-Me]-carba-ENA-modified AON **6** is more stable than [8′*R*-Me]-carba-ENA-modified AON **26**.

**e. Substituent at C6′ Is More Efficient than Substituent at C8′ To Modulate the Nuclease Resistance of Vicinal Phosphate.** From Figure 2, we can see that the modified AONs **34** and **35** which contain the C6′-Me-carba-ENA modifications showed the best stability among all the studied AONs. Given the fact that C6′*R*-OH-carba-ENA-modified AON showed the least nuclease stability among other substituted carba-ENA counterparts,[18] it seems that nuclease resistance of carba-ENA-modified AON is more sensitive to substitution at C6′ than at C8′. This is presumably because of the fact that the C6′ substituent is spatially closer to the phosphate than the C8′ substituent, and thus bestows greater effect during the phosphate recognition process and hydrolysis by the nuclease.

**4.2. The Stereochemical Orientation of the 8′ Substituent Influences the Exonuclease Resistance of the Vicinal Scissile Phosphate.** On the basis of the above comparison, we found the nuclease recognition and subsequent hydrolysis effect imposed by 8′-OH and 8′-Me is significantly dependent on their stereochemical orientation. AON **6** in which 44% of 8′-Me are in the *S* configuration was found to be more stable than AON **26** in which all the 8′-Me are in the *R* configuration, suggesting when 8′-Me points at the 3′-phosphate (8′*S*), it leads to a more positive effect on the nuclease resistance of vicinal phosphate than when it points away from the 3′-phosphate (8′*R*). This stereochemical effect is probably dictated by the spatial proximity of the lipophilic 8′*S* methyl group to the 3′-phosphate compared to that of the 8′*R* methyl group, thus sterically preventing the binding and processing of the phosphate by SVPDE.

Compared to 8′-Me, 8′-OH on carba-ENA exhibits a reverse stereochemical effect on the nuclease resistance: 8′*S*-OH-carba-ENA-modified AON **10** showed a more dramatic decrease of exonuclease resistance than 8′*R*-OH-carba-ENA-modified AON **14**. The destabilization effect caused by 8′*S*-OH on carba-ENA could be attributed to the closure of 8′*S*-OH to vicinal 3′-phosphate. Therefore, the 8′*S*-OH could assist enzymatic cleavage of 3′-phosphate (*P*14) by H-bonding interaction.[52] An interesting observation for SVDPE-mediated digestion of AON **10** is that there is one clear band corresponding to the 13mer formation on the gel (Figure SII 14, Supporting Information), implying that the 8′*S*-OH group can improve the stability of 5′-phosphate (*P*13), putatively by impairing the binding of SVPDE to 5′-phosphate.[52] It is obvious that the destabilization effect on *P*14 surpasses the stabilization effect on *P*13. Hence, 8′*S*-OH on carba-ENA makes modified AON less resistant toward 3′-exonuclease.

**4.3. The Electrostatic Effect of 8′ Substituent Plays an Important Role in Stability Modulation of the Vicinal Phosphate.** 8′*R*-$NH_2$ and 8′*R*-NHPAC on carba-ENA result in a significant decrease in the stability of modified AONs. This destabilization effect is likely attributed to the electrostatics effect. The protonated 8′*R*-amino group, as a zwitterion,

(52) Zhou, C.; Chattopadhyaya, J. *J. Org. Chem.* **2010**, *75*, 2341–2349.

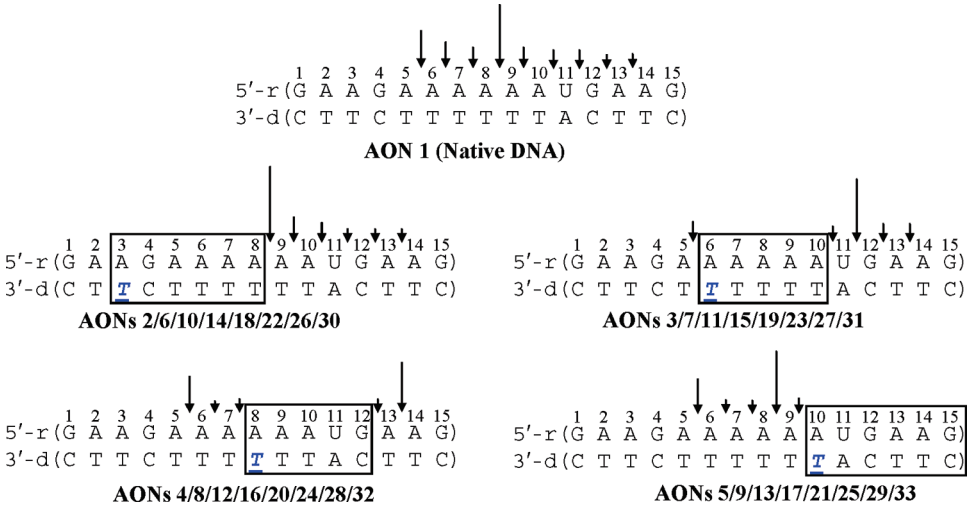


**FIGURE 3.** The *Escherichia coli* RNase H1 promoted cleavage pattern of AONs **1**−**33**:RNA duplexes. Vertical arrows show the RNase H cleavage sites, with the relative length of the arrow indicating the extent of the cleavage. The square boxes show the stretch of the modification, which is resistant to RNase H1 cleavage thereby giving footprints.

could assist binding and interaction between SVPDE and the nucleotide, leading to an unfavorable contribution for enzymatic resistance of the vicinal phosphate. On the other hand, it is known that departure of the 3′-oxyanion is the rate-limiting step for SVPDE-mediated phosphate cleavage.[52] Under the experimental condition, the positively charged 8′*R*-$NH_2$ could exert an induction effect for the stability of the developing 3′-oxyanion, thus assisting it in its departure. As a result, the potential of the scission of 3′*O*−*P*14 bond (Figures 2 and SII 14 in the Supporting Information) is increased. Once the amine was converted into the amide in 8′*R*-NHPAC, which is a better electron-withdrawing group than amino, the cleavage of 3′*O*−*P*14 should be further promoted. This expectation is consistent with the result that [8′*R*-NHPAC]-carba-ENA-modified AON **18** is even less stable then [8′*R*-$NH_2$]-carba-ENA-modified AON **22.**

In summary, the SVPDE resistance can be modulated not only by the stereochemical orientation of the substituents on carbocyclic moiety but also by their intrinsic electrostatic effect. Careful introduction of an electron-donating substituent at the appropriate position of the carbocycle of the carba-ENA or -LNA with correct stereochemistry seems to be an efficient way to design oligonucleotides having high 3′-exonuclease resistance.

**5. RNase H Digestion Study of the Duplexes Formed by Carba-ENA Analogues-Modified AONs with Complementary RNA.** In antisense strategy, RNase H recruitment is a very important property when the modified oligonucleotides are bound to the target RNA in heteroduplex form. So the RNase H-mediated cleavage of the duplexes formed by all modified AON **2**−**33** with complement RNA was studied, applying native DNA (AON **1**) as a reference. As the autoradiographs indicated (Figure SII 15, Supporting Information), all modified AON:RNA hybrids were excellent substrates for RNase H1; however, the cleavage pattern changes, as the site of incorporation of 8′-modified carba-ENA analogues changes, regardless of the modification type of the substituent. In general, the RNase H-elicited cleavage activity (degrading the complementary RNA in the AON:RNA hybrid duplex) was suppressed within a 4−5 base pairs long region that starts from the base opposite to the modified ***T*** nucleotide, toward the 3′-end of the RNA strand. If A8, the preferred cleavage site for native AON **1**:RNA hybrid, is located within the suppressed region, the major cleavage site shifts to the edges of this region (Figure 3). This cleavage pattern is very similar as that of AON:RNA hybrids containing carba-LNA[19] or aza-ENA[15] modifications, so one can effectively engineer a cleavage at a specific site in the RNA strand by properly choosing the position of modification in the complementary antisense strand.[53] Interestingly, this site-specific RNA cleavage property is akin to the hallmark of RNA cleavage in the RNA catalysis.

The RNase H-promoted cleavage rates were determined by autoradiography of gels and subsequently plotting the intact RNA fraction as a function of time (Figure SII 15, Supporting Information). Fitting the degradation curve to single-exponential decay functions gave the digestive rates that are shown as bar plots in Figure 4. It was found that the RNA component in all modified AON:RNA hybrids can be degraded by RNase H with similar or even with better efficiency as the digestion rate of the native counterpart. Comparison of the cleavage rates of the modified AON:RNA hybrid can be summarized in the following conclusions:

(i) ENA (type VIII)-modified hybrids show similar cleavage efficiency as that of the native counterpart. However, the cleavage rate of parent carba-ENA (type I)-modified hybrids is two times better than that of the ENA-modified counterpart, which implies replacement of 2′-*O* of ENA with 2′-$CH_2$ leads to a significant improvement on the RNase H recruitment capability.

(ii) Just like the parent carba-ENA (type I), type VI modification ([8′*R*-$NH_2$]-carba-ENA) also showed a double RNA hydrolysis rate relative to the native counterpart. It is likely that electropositive C8′-$NH_2$ as a zwitterion at the physiological pH presumably plays a role in promoting RNase H digestion, just like its role in assisting 3′-exonuclease-mediated oligo degradation.

(53) Pradeepkumar, P. I.; Chattopadhyaya, J. *J. Chem. Soc., Perkin Trans. 2* **2001**, 2074–2083.

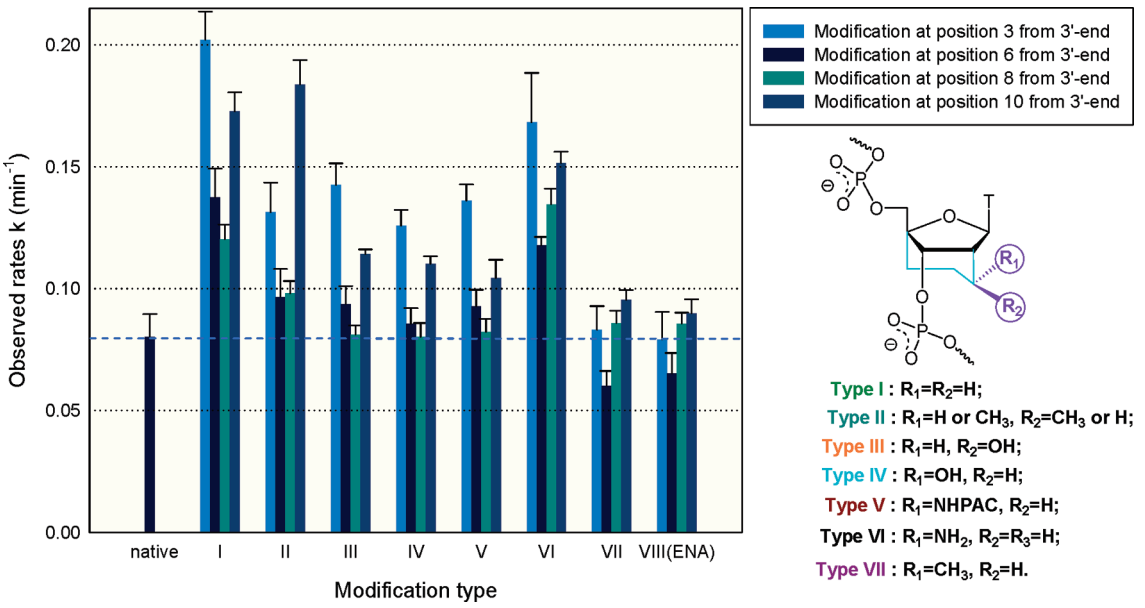


**FIGURE 4.** Bar plots of the observed cleavage rates of the RNase H1-promoted degradation of RNA in AON **1**−**33**:RNA hybrid duplexes. Note that type I modification recruits RNase H at least 2-times better than that of the native.

(iii) For the nonelectropositive group at C8′, type II ([8′-$CH_3$]-carba-ENA)-modified AONs and type IV-modified AONs can mediate the recruitment of RNase H to similar degrees as the native counterpart, suggesting that the nature of the substituent (lipophilic Me versus hydrophilic OH) does not affect the efficiency of RNase H elicitation.

(iv) The RNA cleavage efficiency in the modified AON:RNA hybrids does not depend on the orientation of the substituent at C8′. For example, type III ([8′*S*-OH]-carba-ENA)-modified AONs and type IV ([8′*R*-OH]-carba-ENA)-modified AONs showed the same reaction rate as the native hybrid.

(v) Substitution of carba-ENA or its analogues (types I to VI) at position 3 or 10 (from the 3′-end) of the AON sequence gives a much improved RNA cleavage by RNase H1 in the corresponding heteroduplexes than at any other sites in the sequence. Modification in the middle of the AON strand produces less effective RNase H1 elicitation.

## Conclusions

In this investigation, five 8′-modified carba-ENA derivatives and parent carba-ENA-T have been synthesized through an intramolecular radical cyclization. Biological properties of AONs containing these modifications have been evaluated and compared with that of AONs containing other types of modifications such as LNA, carba-LNA, and ENA. The major conclusions are as follows:

(1) All the carba-ENAs-modified AONs showed improved RNA affinity over their native counterpart. Interestingly, it was found the nature and the steric orientation of the 8′ substituents only slightly affect the $T_m$ values of modified AON:RNA duplexes. One the contrary, carba-ENAs modifications in the AON:DNA homoduplex resulted in significant $T_m$ decrease. Hence, parent carba-ENA and 8′-substituted analogues are highly RNA selective.

(2) The effect of 8′ substituents on the nucleolytic stability of AON was found to greatly depend on the nature and stereochemistry of 8′ substituents on carba-ENA: (i) hydrophobic 8′*S*-Me substituent on carba-ENA increases the nucleolytic stability but 8′*R*-Me lead to a decrease effect; (ii) hydrophilic 8′*R*-OH on carba-ENA had little if any effect on nuclease resistance but 8′*S*-OH resulted in significantly decreased nucleolytic stability; and (iii) zwitterionic 8′-$NH_2$ and 8′-$NH_2$PAC on carba-ENA led to obvious loss on the 3′-exonuclease resistance. Hence, it seems that the electrostatic effect of 8′ substituents contributes to their modulations on nucleolytic stability.

(3) All the carba-ENAs-modified AONs showed better RNase H recruitment capabilities than their native and ENA-modified counterpart. Especially, parent carba-ENA (type I) and [8′*R*-$NH_2$]-carba-ENA (type VI)-modified AONs exhibited double RNA hydrolysis rates relative to the ENA counterpart.

Thus this study shows that carba-ENA and its analogue modified AON fulfill at least three most important criteria for being a winner as potential RNA-directed theraopeutics: (1) desired RNA selectivity; (2) good nuclease stability, and (3) much improved RNase H1 elicitation capability compared to that of the native and ENA-modified AONs.

## Implications

The present study shows that C8′ substituents of carba-ENA impart distinctly different biophysical and biochemical effects on the properties of modified nucleic acids compared to those of C6′ substituents because they have different stereochemical locations, hence interact differently, in the minor groove. Since the C8′ substituent of carba-ENA is located at the bottom and center of the minor groove, and theC6′ substituent of carba-ENA is also at the minor groove (but not at the center) but spatially close to the internucleotidic phosphate, they have different biophysical-chemical effects: it was found that a positively charged amino substituent at the C8′ can improve target affinity and RNase H recruitment capability, whereas the C6′ substituent of carba-ENA

can render a remarkable effect on nuclease resistance in that the C6′*R*-hydrophobic substituent (Me) seems to give the best result. Combining the merits of both C8′ and C6′ substituents in one engineering of a carba-ENA nucleotide, such as a C8′*R*-amino-C6′*R*-Me-carba-ENA moiety, may generate an excellent candidate for AON-based therapeutics, which deserve further investigation in the future. On the other hand, the unique location of C8′ substituents of carba-ENA (at the bottom and center of the minor groove) makes C8′ modified carba-ENA very good chemical models to study the role of electrostatic and steric effect in the self-assembly as well as to probe various biological functions of nucleic acids.

## Experimental Section

Note: All individual reaction steps, workup, and product characterization for compounds **16b**, **17b**, **18a**/**b**, **21b**, **22a**/**b**, **25**, **28**, **29**, **30a**/**b**, **31**, **32**, and ENA are given in the Supporting Information.

**3,5-Di-*O*-benzyl-4-*C*-cyanoethyl-1,2-*O*-isopropylidene-α-D-ribofuranose (8).** $Et_3N$ (15.4 mL, 110.72 mmol) was added dropwise to a solution of **6** (8.66 g, 20.89 mmol), *p*-toluenesulfonyl chloride (7.17 g, 37.61 mmol), and DMAP (255 mg, 2.09 mmol) in anhydrous $CH_2Cl_2$ (290 mL) at 0 °C under $N_2$ atmosphere. The mixture was allowed to warm to room temperature followed by stirring overnight at this temperature. The reaction was quenched with saturated aqueous $NaHCO_3$ and the obtained mixture was partitioned between $CH_2Cl_2$ and water, then the aqueous layer was extracted again with $CH_2Cl_2$. The combined organic layer was dried over $MgSO_4$ and evaporated to give tosylate **7**. Compound **7** was dissolved in anhydrous DMF (73 mL) and tetrabutylammonium cyanide (14.02 g, 52.23 mmol) was added. The obtained solution was stirred at room temperature for 2.5 days, then warmed to 35 °C followed by stirring at this temperature for 1 day. After evaporation of solvent, the residue was dissolved in $CH_2Cl_2$ and saturated aqueous $NaHCO_3$. The organic layer was separated and the aqueous layer was extracted again with $CH_2Cl_2$. The combined organic layer was dried over $MgSO_4$ and concentrated. The residue was purified by column chromatography on silica gel (4−6% acetone in petroleum ether, v/v) to obtain **8** (6.85 g, 77.4% in two steps) as a light yellow syrup. $^1$H NMR (500 MHz, $CDCl_3$) $\delta$ 7.34−7.23 (10H, m, aromatic), 5.73 (1H, d, $J_{1,2}$ = 4.0 Hz, H1), 4.75 (1H, d, $J_{gem}$ = 12.0 Hz, C$\underline{H_2}$Bn), 4.60 (1H, dd, $J_{1,2}$ = 4.0 Hz, $J_{2,3}$ = 5.0 Hz, H2), 4.52 (1H, d, $J_{gem}$ = 12.0 Hz, C$\underline{H_2}$Bn), 4.48 (1H, d, $J_{gem}$ = 12.0 Hz, C$\underline{H_2}$Bn), 4.43 (1H, d, $J_{gem}$ = 12.0 Hz, C$\underline{H_2}$Bn), 4.00 (1H, d, $J_{2,3}$ = 5.0 Hz, H3), 3.37 (1H, d, $J_{gem}$ = 10.0 Hz, H5), 3.25 (1H, d, $J_{gem}$ = 10.0 Hz, H5′), 2.59 (2H, m, H7 and H6), 2.43 (1H, m, H7′), 1.91 (1H, m, H6′), 1.58 (3H, s, $CH_3$), 1.31 (3H, s, $CH_3$). $^{13}$C NMR (125 MHz, $CDCl_3$) $\delta$ 137.6 (2 × $C_{ipso}$-Bn), 128.4−127.7 (aromatic), 120.5 (isopropyl), 113.2 (CN), 104.3 (C1), 85.1 (C4), 79.3 (C3), 78.5 (C2), 73.6 (C$\underline{H_2}$Bn), 73.0 (C5), 72.4 (C$\underline{H_2}$Bn), 27.9 (C6), 26.5 (C$\underline{H_3}$), 25.8 (C$\underline{H_3}$), 11.9 (C7). MALDI-TOF $m/z$ $[C_{25}H_{29}NO_5 + Na]^+$ found 446.194, calcd 446.200.

**1-(2-*O*-Acetyl-3,5-*O*-benzyl-4-*C*-cyanoethyl-β-D-ribofuranosyl)-thymine (10).** Compound **8** (4.76 g, 11.24 mmol) was dissolved in acetic anhydride (6.3 mL, 67.44 mmol) and acetic acid (63 mL). This solution was cooled to 10 °C, to which trifilic acid (100 μL, 1.12 mmol) was added dropwise, and the obtained mixture was stirred at this temperature for 1 h. The reaction was quenched with saturated aqueous $NaHCO_3$ and extracted with $CH_2Cl_2$. The organic layer was dried over $MgSO_4$ and evaporated to give crude product **9**. The crude product, after coevaporation with toluene twice, was dissolved in anhydrous MeCN (146 mL), to which thymine (2.12 g, 16.85 mmol) and *N*,*O*-bis(trimethylsilyl)-acetamide (7.5 mL, 30.35 mmol) was added under $N_2$ followed by reflux for 30 min until the suspension became a clear solution. Then the solution was cooled to room temperature and TMSOTf (2.5 mL, 14.05 mmol) was added dropwise. The obtained mixture was refluxed overnight followed by quenching with saturated aqueous $NaHCO_3$ and extracted with $CH_2Cl_2$. The organic layer was dried over $MgSO_4$ and concentrated. The residue was purified by column chromatography on silica gel (20−33% acetone in petroleum ether, v/v) to obtain **10** (5.07 g, 84.5% in two steps) as a white foam. $^1$H NMR (600 MHz, $CDCl_3$) $\delta$ 9.09 (1H, s, H3), 7.38−7.26 (11H, m, aromatic and H6), 6.05 (1H, d, $J_{1′,2′}$ = 4.8 Hz, H1′), 5.45 (1H, dd, $J_{1′,2′}$ = 4.8 Hz, $J_{2′,3′}$ = 6.0 Hz, H2′), 4.62 (1H, d, $J_{gem}$ = 11.4 Hz, C$\underline{H_2}$Bn), 4.52 (1H, d, $J_{gem}$ = 11.4 Hz, C$\underline{H_2}$Bn), 4.47 (1H, d, $J_{gem}$ = 11.4 Hz, C$\underline{H_2}$Bn), 4.43 (1H, d, $J_{gem}$ = 11.4 Hz, C$\underline{H_2}$Bn), 4.42 (1H, d, $J_{2′,3′}$ = 6.0 Hz, H3′), 3.62 (1H, d, $J_{gem}$ = 9.6 Hz, H5′), 3.37 (1H, d, $J_{gem}$ = 9.6 Hz, H5″), 2.55 (1H, m, H7′), 2.41 (1H, m, H7″), 2.21 (1H, m, H6′), 2.10 (3H, s, acetyl-C$\underline{H_3}$), 1.85 (1H, m, H7″), 1.60 (3H, s, thymine-C$\underline{H_3}$). $^{13}$C NMR (150 MHz, $CDCl_3$) $\delta$ 170.3 (C=O, acetyl), 163.9 (C4), 150.7 (C2), 137.3, 137.2 (2 × $C_{ipso}$-Bn), 136.3 (C6), 129.0−128.1 (aromatic), 120.3 (CN), 111.9 (C5), 88.1 (C1′), 86.3 (C4′), 78.6 (C3′), 74.9 (C2′), 74.8, 73.9 (C$\underline{H_2}$Bn), 72.8 (C5′), 28.6 (C6′), 21.0 (C$\underline{H_3}$, acetyl), 12.4 (C$\underline{H_3}$-thymine), 12.2 (C7′). MALDI-TOF $m/z$ $[C_{29}H_{31}N_3O_7 + H]^+$ found 534.224, calcd 534.223.

**1-(3,5-*O*-Benzyl-4-*C*-cyanoethyl-2-*O*-hydroxyl-β-D-ribofuranosyl)-thymine (11).** Compound **10** (2.52 g, 4.72 mmol) was dissolved in methanol (13 mL) and methylamine solution (95 mL). The mixture was stirred in an ice bath for 1 h. After evaporation of solvent, the obtained residue was purified by column chromatography on silica gel (1% methanol in $CH_2Cl_2$, v/v) to obtain **11** (2.19 g, 94.7%) as white foam. $^1$H NMR (500 MHz, $CDCl_3$) $\delta$ 9.10 (1H, s, H3), 7.39−7.26 (11H, m, aromatic and H6), 5.84 (1H, d, $J_{1′,2′}$ = 5.5 Hz, H1′), 4.78 (1H, d, $J_{gem}$ = 11.5 Hz, C$\underline{H_2}$Bn), 4.61 (1H, d, $J_{gem}$ = 11.5 Hz, C$\underline{H_2}$Bn), 4.55 (1H, d, $J_{gem}$ = 11.5 Hz, C$\underline{H_2}$Bn), 4.50 (1H, d, $J_{gem}$ = 11.5 Hz, C$\underline{H_2}$Bn), 4.41 (1H, dd, $J_{1′,2′}$ = 5.5 Hz, $J_{2′,3′}$ = 6.0 Hz, $J_{2′,OH}$ = 7.0 Hz, H2′), 4.22 (1H, d, $J_{2′,3′}$ = 6.0 Hz, H3′), 3.60 (1H, d, $J_{gem}$ = 10.0 Hz, H5′), 3.53 (1H, d, $J_{2′,OH}$ = 7.0 Hz, 2′-OH), 3.40 (1H, d, $J_{gem}$ = 10.0 Hz, H5″), 2.52 (1H, m, H7′), 2.39 (1H, m, H7″), 2.29 (1H, m, H6′), 1.84 (1H, m, H6″), 1.61 (3H, s, thymine-C$\underline{H_3}$). $^{13}$C NMR (150 MHz, $CDCl_3$) $\delta$ 164.0 (C4), 151.2 (C2), 137.3, 137.2 (2 × $C_{ipso}$-Bn), 136.4 (C6), 129.1−128.1 (aromatic), 120.4 (CN), 111.5 (C5), 90.3 (C1′), 86.2 (C4′), 79.8 (C3′), 75.0 (C2′), 74.9, 74.1 (C$\underline{H_2}$Bn), 73.1 (C5′), 28.8 (C6′), 12.5 (C$\underline{H_3}$-thymine), 12.2 (C7′). MALDI-TOF $m/z$ $[C_{27}H_{29}N_3O_6 + H]^+$ found 492.215, calcd 492.213.

**1-(3,5-*O*-Benzyl-4-*C*-propionaldehyde-2-*O*-hydroxyl-β-D-ribofuranosyl)thymine *O*-Benzyl Oxime (12).** DIBALH (11.5 mL, 11.5 mmol, 1.0 M solution in toluene) was added dropwise to a solution of **11** (1.41 g, 2.87 mmol) in anhydrous $CH_2Cl_2$ (29 mL) over 30 min at −78 °C. After being stirred at the same temperature for 2 h under nitrogen atmosphere, the mixture was quenched with methanol at −78 °C, followed by water. The mixture was allowed to warm to room temperature until a precipitate was formed, which was filtered though Celite. The filtrate was washed with 10% aqueous acetic acid, saturated aqueous $NaHCO_3$, and brine. The organic layer was dried over $MgSO_4$ and concentrated to give crude aldehyde as an intermediate. The crude aldehyde was dissolved in anhydrous $CH_2Cl_2$ (29 mL) and anhydrous pyridine (1.4 mL, 17.22 mmol), to which *O*-benzyl hydroxylamine hydrochloride (916 mg, 5.74 mmmol) was added. After refluxing for 1 h, the mixture was cooled to room temperature and saturated aqueous $NaHCO_3$ was added. The organic layer was separated, dried over $MgSO_4$, and evaporated. The residue was subjected to short column chromatography over silica gel (0.9−1.2% methanol in $CH_2Cl_2$, v/v) to give **12** (1.04 g, 60.6% in two steps) as the mixture of *Z* and *E* isomers. **Isomer I:** $^1$H NMR (500 MHz, $CDCl_3$) $\delta$ 8.14 (1H, s, H3), 7.44 (1H, t, $J_{7″,8′}$ = 5.4 Hz, $J_{7″,8′}$ = 5.4 Hz, H8′), 7.37−7.26 (16H, m, aromatic and H6), 5.89 (1H, d, $J_{1′,2′}$ = 6.0 Hz, H1′), 5.05 (2H, s, NOC$\underline{H_2}$Bn),

4.68 (1H, d, $J_{gem}$ = 11.5 Hz, CH$_2$Bn), 4.65 (1H, d, $J_{gem}$ = 11.5 Hz, CH$_2$Bn), 4.52 (1H, d, $J_{gem}$ = 11.5 Hz, CH$_2$Bn), 4.49 (1H, d, $J_{gem}$ = 11.5 Hz, CH$_2$Bn), 4.34 (1H, m, $J_{1',2'}$ = 6.0 Hz, $J_{2',3'}$ = 6.0 Hz, $J_{2',OH}$ = 8.5 Hz, H2′), 4.16 (1H, d, $J_{2',3'}$ = 6.0 Hz, H3′), 3.61 (1H, d, $J_{gem}$ = 10.0 Hz, H5′), 3.40 (1H, d, $J_{gem}$ = 10.0 Hz, H5″), 2.90 (1H, d, $J_{2',OH}$ = 8.5 Hz, 2′-OH), 2.38 (1H, m, H7′), 2.22 (1H, m, H7″), 2.12 (1H, m, H6′), 1.70 (1H, m, H6″), 1.61 (3H, d, $J_{6,CH_3}$ = 0.6 Hz, thymine-CH$_3$). $^{13}$C NMR (150 MHz, CDCl$_3$) $\delta$ 163.2 (C4), 150.6 (C8′), 150.5 (C2), 137.7, 137.1, 136.7 (3 × C$_{ipso}$-Bn), 135.8 (C6), 128.8−127.6 (aromatic), 111.1 (C5), 88.6 (C1′), 86.7 (C4′), 80.2 (C3′), 75.6 75.1 (2 × CH$_2$Bn), 74.7 (C2′), 73.7 (CH$_2$Bn), 73.5 (C5′), 29.1 (C6′), 24.0 (C7′), 12.1 (CH$_3$-thymine). **Isomer II:** $^1$H NMR (500 MHz, CDCl$_3$) $\delta$ 8.20 (1H, s, H3), 7.39−7.26 (16H, m, aromatic and H6), 6.68 (1H, t, $J_{7',8'}$ = 5.5 Hz, $J_{7'',8'}$ = 5.5 Hz, H8′), 5.87 (1H, d, $J_{1',2'}$ = 6.0 Hz, H1′), 5.05 (2H, s, NOCH$_2$Bn), 4.68 (1H, d, $J_{gem}$ = 11.5 Hz, CH$_2$Bn), 4.63 (1H, d, $J_{gem}$ = 11.5 Hz, CH$_2$Bn), 4.52 (1H, d, $J_{gem}$ = 11.5 Hz, CH$_2$Bn), 4.48 (1H, d, $J_{gem}$ = 11.5 Hz, CH$_2$Bn), 4.33 (1H, dd, $J_{1',2'}$ = 6.0 Hz, $J_{2',3'}$ = 6.0 Hz, $J_{2',OH}$ = 7.5 Hz, H2′), 4.17 (1H, d, $J_{2',3'}$ = 6.0 Hz, H3′), 3.63 (1H, d, $J_{gem}$ = 10.0 Hz, H5′), 3.41 (1H, d, $J_{gem}$ = 10.0 Hz, H5″), 3.93 (1H, d, $J_{2',OH}$ = 7.5 Hz, 2′-OH), 2.45 (2H, m, H7′ and H7″), 2.08 (1H, m, H6′), 1.71 (1H, m, H6″), 1.60 (3H, s, thymine-CH$_3$). $^{13}$C NMR (125 MHz, CDCl$_3$) $\delta$ 163.3 (C4), 151.5 (C8′), 150.6 (C2), 138.0, 137.2, 136.8 (3 × C$_{ipso}$-Bn), 135.9 (C6), 128.8−127.6 (aromatic), 111.1 (C5), 88.9 (C1′), 86.8 (C4′), 80.0 (C3′), 75.9, 75.0 (2 × CH$_2$Bn), 74.8 (C2′), 73.7 (CH$_2$Bn), 73.3 (C5′), 28.8 (C6′), 20.4 (C7′), 12.1 (CH$_3$-thymine). MALDI-TOF $m/z$ [C$_{34}$H$_{37}$N$_3$O$_7$ + H]$^+$ found 600.272, calcd 600.270.

**1-(3,5-*O*-Benzyl-2-*O*-phenoxythiocarbonyl-4-*C*-propionaldehyde-β-D-ribofuranosyl)thymine *O*-Benzyl Oxime (13).** To a solution of **12** (1.13 g, 1.89 mmol) in anhydrous pyridine (19 mL) was added dropwise phenyl chlorothionoformate (0.31 mL, 2.27 mmol) in an ice bath under N$_2$. The mixture was stirred for 30 min in the ice bath, then stirred for a further 2 h at room temperature followed by quenching with methanol. After the mixture was stirred for 30 min, the solvent was removed. The residue was dissolved in CH$_2$Cl$_2$ and washed with saturated aqueous NaHCO$_3$, and then the aqueous layer was extracted with CH$_2$Cl$_2$ twice. The combined organic layer was dried over MgSO$_4$ and evaporated. The residue was purified by column chromatography on silica gel (11−17% acetone in petroleum ether, v/v) to obtain **13** (1.23 g, 88.7%) as the mixture of *Z* and *E* isomers. **Isomer I:** $^1$H NMR (500 MHz, CDCl$_3$) $\delta$ 8.23 (1H, s, H3), 7.44 (1H, d, $J_{6,CH_3}$ = 1.2 Hz, H6), 7.41−7.26 (19H, m, aromatic and H8′), 7.00 (2H, dd, aromatic), 6.35 (1H, d, $J_{1',2'}$ = 6.0 Hz, H1′), 5.95 (1H, t, $J_{1',2'}$ = 6.0 Hz, $J_{2',3'}$ = 6.0 Hz, H2′), 5.04 (2H, s, NOCH$_2$Bn), 4.74 (1H, d, $J_{gem}$ = 11.0 Hz, CH$_2$Bn), 4.54 (1H, d, $J_{2',3'}$ = 6.0 Hz, H3′), 4.53 (1H, d, $J_{gem}$ = 11.0 Hz, CH$_2$Bn), 4.52 (2H, s, CH$_2$Bn), 3.67 (1H, d, $J_{gem}$ = 10.0 Hz, H5′), 3.43 (1H, d, $J_{gem}$ = 10.0 Hz, H5″), 2.37 (1H, m, H7′), 2.22 (1H, m, H7″), 2.05 (1H, m, H6′), 1.74 (1H, m, H6″), 1.54 (3H, d, $J_{6,CH_3}$ = 1.2 Hz, thymine-CH$_3$). $^{13}$C NMR (125 MHz, CDCl$_3$) $\delta$ 194.4 (C═S), 163.3 (C4), 153.4 (C$_{ipso}$-Bn), 150.6 (C8′), 150.2 (C2), 137.7, 137.2, 137.0 (3 × C$_{ipso}$-Bn), 135.8 (C6), 129.6−126.8, 121.7 (aromatic), 111.6 (C5), 87.3 (C4′), 85.6 (C1′), 82.8 (C2′), 78.1 (C3′), 75.6, 75.0, 73.8 (3 × CH$_2$Bn), 73.4 (C5′), 29.1 (C6′), 24.1 (C7′), 12.1 (CH$_3$-thymine). **Isomer II:** $^1$H NMR (600 MHz, CDCl$_3$) $\delta$ 9.37 (1H, s, H3), 7.43 (1H, s, H6), 7.42−7.30 (18H, m, aromatic), 7.00 (2H, dd, aromatic), 6.68 (1H, t, $J_{7',8'}$ = 5.4 Hz, $J_{7'',8'}$ = 5.4 Hz, H8′), 6.39 (1H, d, $J_{1',2'}$ = 6.0 Hz, H1′), 5.93 (1H, t, $J_{1',2'}$ = 6.0 Hz, $J_{2',3'}$ = 6.0 Hz, H2′), 5.10 (2H, s, NOCH$_2$Bn), 4.76 (1H, d, $J_{gem}$ = 11.4 Hz, CH$_2$Bn), 4.60 (1H, d, $J_{2',3'}$ = 6.0 Hz, H3′), 4.55 (1H, d, $J_{gem}$ = 11.4 Hz, CH$_2$Bn), 4.52 (2H, s, CH$_2$Bn), 3.72 (1H, d, $J_{gem}$ = 10.2 Hz, H5′), 3.46 (1H, d, $J_{gem}$ = 10.2 Hz, H5″), 2.44 (2H, m, H7′ and H7″), 2.04 (1H, m, H6′), 1.75 (1H, m, H6″), 1.47 (3H, s, thymine-CH$_3$). $^{13}$C NMR (125 MHz, CDCl$_3$) $\delta$ 195.0 (C═S), 164.5 (C4), 153.7 (C$_{ipso}$-Bn), 152.0 (C8′), 151.0 (C2), 138.2, 137.6, 137.4 (3 × C$_{ipso}$-Bn), 136.4 (C6), 130.2−127.4, 122.2 (aromatic), 112.2 (C5), 87.7 (C4′), 85.8 (C1′), 83.3 (C2′), 78.4 (C3′), 76.2, 75.4, 74.1 (3 × CH$_2$Bn), 73.5 (C5′), 29.1 (C6′), 20.9 (C7′), 12.6 (CH$_3$-thymine). MALDI-TOF $m/z$: [C$_{41}$H$_{41}$N$_3$O$_8$S + H]$^+$ found 736.270, calcd 736.269.

**(1*R*,3*R*,4*R*,5*R*,8*S*)-8-Benzyloxy-1-benzyloxymethyl-5-benzyloxyamino-3-(thymin-1-yl)-2-oxa-bicyclo[3.2.1]octane (14).** Compound **13** (910 mg, 1.237 mmol) was dissolved in anhydrous toluene (130 mL) then the solution was purged with N$_2$ for 40 min. The mixture was refluxed, Bn$_3$SnH (0.8 mL in 20 mL dry toluene) and AIBN (40 mg in 10 mL dry toluene) were added dropwise in 5 h, then the mixture continued to reflux for 1 h. The mixture was cooled to room temperature and solvent was evaporated. The residue was chromatographed on silica gel (18−30% in ethyl acetate in cyclohexane, v/v) to give **14** (433 mg, 60.1%) as a white foam. $^1$H NMR (500 MHz, CDCl$_3$) $\delta$ 8.20 (1H, s, H3), 8.00 (1H, d, $J_{6,CH_3}$ = 1.0 Hz, H6), 7.39−7.26 (15H, m, aromatic), 5.99 (1H, s, H1′), 5.58 (1H, s, NH), 4.83 (1H, d, $J_{gem}$ = 11.5 Hz, CH$_2$Bn), 4.80 (1H, d, $J_{gem}$ = 11.5 Hz, CH$_2$Bn), 4.61 (1H, d, $J_{gem}$ = 11.5 Hz, CH$_2$Bn), 4.57 (1H, d, $J_{gem}$ = 11.5 Hz, CH$_2$Bn), 4.52 (1H, d, $J_{gem}$ = 11.5 Hz, CH$_2$Bn), 4.44 (1H, d, $J_{gem}$ = 11.5 Hz, CH$_2$Bn), 4.25 (1H, d, $J_{2',3'}$ = 5.0 Hz, H3′), 3.69 (1H, d, $J_{gem}$ = 11.0 Hz, H5′), 3.56 (1H, m, $J_{2',8'}$ = 3.5 Hz, $J_{7',8'}$ = 5.0 Hz, $J_{7'',8'}$ = 11.5 Hz, H8′), 3.54 (1H, d, $J_{gem}$ = 11.0 Hz, H5″), 2.82 (1H, d, $J_{2',8'}$ = 3.5 Hz, $J_{2',3'}$ = 5.0 Hz, H2′), 1.86 (1H, m, H6′), 1.80 (1H, m, H7′), 1.61 (3H, d, $J_{6,CH_3}$ = 1.0 Hz, thymine-CH$_3$), 1.40 (1H, m, H6′), 1.38 (1H, m, H7″). $^{13}$C NMR (125 MHz, CDCl$_3$) $\delta$ 163.8 (C4), 149.7 (C2), 138.1, 137.5, 137.4 (C$_{ipso}$-Bn), 136.5 (C6), 128.6−127.5 (aromatic), 109.3 (C5), 84.6 (C4′), 84.4 (C1′), 76.5, 73.6 (2 × CH$_2$Bn), 73.2 (C3′), 71.9 (CH$_2$Bn), 70.2 (C5′), 53.5 (C8′), 44.7 (C2′), 26.2 (C6′), 22.1 (C7′), 11.9 (CH$_3$-thymine). MALDI-TOF $m/z$ [C$_{34}$H$_{37}$N$_3$O$_6$ + Na]$^+$ found 606.258, calcd 606.257.

**(1*R*,3*R*,4*R*,5*R*,8*S*)-8-Benzyloxy-1-benzyloxymethyl-5-trifluoroacetamino-3-(thymin-1-yl)-2-oxa-bicyclo[3.2.1]octane (16a).** To a solution of **14** (110 mg, 0.188 mmol) in anhydrous methanol (4.0 mL) were added 10% Pd/C (94 mg) and ammonium formate (475 mg, 7.54 mmol) under nitrogen. The mixture was stirred for 8 h at room temperature. The suspension was filtered through a pad of Celite. The filtrate was concentrated and dried over vacuum pump. The obtained crude amine **15** was dissolved in a mixture of anhydrous CH$_2$Cl$_2$ (3.8 mL) and pyridine (0.12 mL, 1.50 mmol) and cooled to 0 °C, to which trifluoroacetic anhydride (0.1 mL, 0.752 mmol) was added dropwise over 5 min. Then the reaction mixture was allowed to warm to room temperature and stirred at this temperature for 2 h, followed by quenching with crushed ice and diluted with CH$_2$Cl$_2$. The aqueous layer was extracted with CH$_2$Cl$_2$ twice. The organic layers were combined, dried over MgSO$_4$, and concentrated. The residue was purified by column chromatography on silica gel (0.6−0.8% methanol in CH$_2$Cl$_2$, v/v) to obtain **16a** (65 mg, 60.0% in two steps) as a white foam. $^1$H NMR (500 MHz, CDCl$_3$) $\delta$ 8.79 (1H, s, H3), 7.89 (1H, d, $J_{6,CH_3}$ = 1.5 Hz, H6), 7.65 (1H, d, $J_{8',NH}$ = 6.5 Hz, 8′-NH), 7.40−7.27 (10H, m, aromatic), 5.92 (1H, s, H1′), 4.71 (1H, d, $J_{gem}$ = 11.5 Hz, CH$_2$Bn), 4.59 (1H, d, $J_{gem}$ = 11.5 Hz, CH$_2$Bn), 4.54 (1H, d, $J_{gem}$ = 11.5 Hz, CH$_2$Bn), 4.53 (1H, d, $J_{gem}$ = 11.5 Hz, CH$_2$Bn), 4.46 (1H, m, $J_{NH,8'}$ = 6.5 Hz, $J_{7',8'}$ = 6.0 Hz, $J_{7'',8'}$ = 11.0 Hz, H8′), 4.27 (1H, d, $J_{2',3'}$ = 5.0 Hz, H3′), 3.74 (1H, d, $J_{gem}$ = 10.5 Hz, H5′), 3.59 (1H, d, $J_{gem}$ = 10.5 Hz, H5″), 2.63 (1H, d, $J_{2',3'}$ = 5.0 Hz, H2′), 2.34 (1H, m, $J_{6',7'}$ = 6.0 Hz, $J_{7',8'}$ = 6.0 Hz, $J_{7',7''}$ = 13.0 Hz, H7′), 1.96 (1H, ddd, $J_{6',7'}$ = 6.0 Hz, $J_{6',7''}$ = 13.0 Hz, $J_{6',6''}$ = 13.0 Hz, H6′), 1.63 (1H, m, $J_{6',7''}$ = 6.0 Hz, $J_{6'',7''}$ = 6.5 Hz, $J_{7'',8'}$ = 11.0 Hz, $J_{7',7''}$ = 13.0 Hz, H7″), 1.51 (1H, dd, $J_{6'',7''}$ = 6.5 Hz, $J_{6',6''}$ = 13.0 Hz, H6″), 1.46 (3H, d, $J_{6,CH_3}$ = 1.5 Hz, thymine-CH$_3$). $^{13}$C NMR (125 MHz, CDCl$_3$) $\delta$ 164.0 (C4), 157.2 (CF$_3$CO), 150.3 (C2), 137.3, 137.0 (2 × C$_{ipso}$-Bn), 135.4 (C6), 128.7−127.8 (aromatic), 115.8 (CF$_3$CO), 110.2 (C5), 84.9 (C4′), 84.1 (C1′), 73.6 (CH$_2$Bn), 72.8 (C3′), 72.4 (CH$_2$Bn), 69.8 (C5′), 47.4 (C2′), 44.4 (C8′), 26.1 (C6′), 24.1 (C7′), 11.9 (CH$_3$-thymine). MALDI-TOF $m/z$ [C$_{29}$H$_{30}$F$_3$N$_3$O$_6$ + H]$^+$ found 574.212, calcd 574.216.

**(1*R*,3*R*,4*R*,5*R*,8*S*)-1-(4,4′-Dimethoxytrityloxymethyl)-8-hydroxyl-5-trifluoroacetamino-3-(thymin-1-yl)-2-oxa-bicyclo[3.2.1]octane (17a).** A mixture of 20% Pd(OH)$_2$/C (100 mg), **16a** (95 mg,

0.166 mmol) in ethanol (6.6 mL), and cyclohexene (13.2 mL) was reflux overnight. Then the suspension was filtered through a pad of Celite. The filtrate was concentrated and dried. The residue was coevaporated twice with dry pyridine and dissolved in the same solvent (1.7 mL), to which 4,4′-dimethoxytrityl chloride (69 mg, 0.202 mmol) was added, and stirred overnight at room temperature. Then solvent was removed and the obtained residue was chromatographed on silica gel (0−0.6% methanol in $CH_2Cl_2$ containing 1% pyridine, v/v) to obtain **17a** (35 mg, 30.3% in two steps) as a white foam. $^1$H NMR (600 MHz, $CDCl_3$ + $d^4$-MeOH) $\delta$ 8.24 (1H, d, $J_{8',NH}$ = 6.0 Hz, 8′-NH), 7.90 (1H, s, H6), 7.43−6.84 (13H, m, aromatic), 5.85 (1H, s, H1′), 4.63 (1H, d, $J_{2',3'}$ = 5.4 Hz, H3′), 4.52 (1H, m, $J_{2',8'}$ = 2.5 Hz, $J_{8',NH}$ = 6.0 Hz, $J_{7',8'}$ = 6.0 Hz, $J_{7'',8'}$ = 11.5 Hz, H8′), 3.79 (6H, s, 2 × OC$H_3$), 3.35 (1H, d, $J_{gem}$ = 10.8 Hz, H5′), 3.28 (1H, d, $J_{gem}$ = 10.8 Hz, H5″), 2.58 (1H, d, $J_{2',8'}$ = 2.5 Hz, $J_{2',3'}$ = 5.4 Hz, H2′), 2.16 (2H, m, $J_{7',8'}$ = 6.0 Hz, $J_{6',7'}$ = 6.0 Hz, $J_{7',7''}$ = 13.8 Hz, H7′ and 3′-OH), 1.87 (1H, ddd, $J_{6',7'}$ = 6.0 Hz, $J_{6',7''}$ = 12.6 Hz, $J_{6',6''}$ = 13.8 Hz, H6′), 1.61 (1H, m, $J_{7'',8'}$ = 11.5 Hz, $J_{6'',7''}$ = 6.6 Hz, $J_{6',7''}$ = 12.6 Hz, $J_{7',7''}$ = 13.8 Hz, H7″), 1.45 (1H, dd, $J_{6'',7''}$ = 6.6 Hz, $J_{6',6''}$ = 13.8 Hz, H6″), 1.29 (3H, s, thymine-C$H_3$). $^{13}$C NMR (125 MHz, $CDCl_3$) $\delta$ 164.3 (C4), 158.7, 158.6 (2 × OMe-$C_{ispo}$), 157.5 ($CF_3CO$), 150.8 (C2), 144.3, 135.5, 135.3 (DMTr-$C_{ispo}$), 135.2 (C6), 130.1−124.0 (aromatic), 115.8 ($CF_3CO$), 113.3 (aromatic), 110.4 (C5), 86.6 (DMTr-C), 85.8 (C4′), 84.2 (C1′), 66.5 (C3′), 63.3 (C5′), 55.2 (2 × OMe), 49.9 (C2′), 44.3 (C8′), 25.8 (C6′), 23.8 (C7′), 11.9 ($CH_3$-thymine). MALDI-TOF $m/z$ [$C_{36}H_{36}F_3N_3O_8$ + Na]$^+$ found 718.235, calcd 718.235.

**(1*R*,3*R*,4*R*,8*S*)-8-Benzyloxy-1-benzyloxymethyl-5-one-3-(thymin-1-yl)-2-oxa-bicyclo[3.2.1]octane (19).** The crude amine **15** (0.43 mmol) was dissolved in dry methanol (2.6 mL) and dry THF (0.4 mL), to which was added 3,5-di-*tert*-butyl-1,2-benzoquinone (114 mg, 0.516 mmol). The mixture was stirred at 40 °C for 10 h, then $H_2O$ (0.72 mL) and oxalic acid (68 mg, 0.54 mmol) were added followed by stirring at 40 °C overnight. Then additional $H_2O$ (5 mL) was added and extracted with EtOAc three times. The organic layer was dried over $MgSO_4$ and evaporated to dryness. The residue was applied to column chromatography on silica gel (0.5−2% methanol in $CH_2Cl_2$, v/v) to give compound **19** (102 mg, 50% in two steps). $^1$H NMR (500 MHz, $CDCl_3$) $\delta$ 8.54 (1H, s, H3), 8.00 (1H, d, $J_{6,CH_3}$ = 1.5 Hz, H6), 7.38−7.26 (10H, m, aromatic), 6.07 (1H, s, H1′), 4.68 (1H, d, $J_{gem}$ = 11.5 Hz, C$H_2$Bn), 4.63 (1H, d, $J_{2,3}$ = 5.5 Hz, H3′), 4.62 (1H, d, $J_{gem}$ = 11.5 Hz, C$H_2$Bn), 4.56 (1H, d, $J_{gem}$ = 11.5 Hz, C$H_2$Bn), 4.42 (1H, d, $J_{gem}$ = 11.5 Hz, C$H_2$Bn), 3.87 (1H, d, $J_{gem}$ = 11.0 Hz, H5′), 3.65 (1H, d, $J_{gem}$ = 11.0 Hz, H5″), 3.32 (1H, d, $J_{2',3'}$ = 5.5 Hz, H2′), 2.61 (1H, m, $J_{6'',7'}$ = 9.0 Hz, $J_{6',7'}$ = 10.5 Hz, $J_{7',7''}$ = 16.5 Hz, H7′), 2.52 (1H, dd, $J_{6',7''}$ = 7.5 Hz, $J_{7',7''}$ = 16.5 Hz, H7″), 2.15 (1H, m, $J_{6',7''}$ = 7.5 Hz, $J_{6',7'}$ = 10.5 Hz, $J_{6',6''}$ = 13.5 Hz, H6′), 1.91 (1H, dd, $J_{6'',7'}$ = 9.0 Hz, $J_{6',6''}$ = 13.5 Hz, H6″), 1.44 (3H, d, $J_{6,CH_3}$ = 1.5 Hz, thymine-C$H_3$). $^{13}$C NMR (125 MHz, $CDCl_3$) $\delta$ 204.0 (C8′), 162.6 (C4), 148.7 (C2), 136.0, 135.6 (aromatic), 134.3 (C6), 127.7−126.9 (aromatic), 109.1 (C5), 84.1 (C4′), 83.4 (C1′), 75.1 (C3′), 72.7 (C$H_2$Bn), 71.1 (C$H_2$Bn), 68.6 (C5′), 58.4 (C2′), 33.5 (C7′), 27.0 (C6′), 10.8 (thymine-C$H_3$). MALDI-TOF $m/z$ [$C_{27}H_{28}N_2O_6$ + H]$^+$ found 477.203, calcd 477.202.

**(1*R*,3*R*,4*R*,5*S*,8*S*)-8-Benzyloxy-1-benzyloxymethyl-5-hydroxy-3-(thymin-1-yl)-2-oxa-bicyclo[3.2.1]octane (20a) and (1*R*,3*R*,4*R*,5*R*,8*S*)-8-Benzyloxy-1-benzyloxymethyl-5-hydroxy-3-(thymin-1-yl)-2-oxa-bicyclo[3.2.1]octane (20b).** $NaBH_4$ (59 mg, 1.55 mmol) was added to a solution of **19** (185 mg, 0.338 mmol) in ethanol (10 mL). The mixture was stirred at room temperature for 4 h followed by quenching with acetone. After evaporation of solvent, the residue was purified by column chromatography on silica gel (1.1−5% methanol in $CH_2Cl_2$, v/v) to obtain two diastereomers **20a** (112 mg, 69.2%) and **20b** (30 mg, 18.6%) as a white foam. **20a:** $^1$H NMR (500 MHz, $CDCl_3$) $\delta$ 8.33 (1H, s, H3), 7.99 (1H, d, $J_{6,CH_3}$ = 1.0 Hz, H6), 7.46−7.25 (10H, m, aromatic), 5.57 (1H, s, H1′), 4.73 (1H, d, $J_{gem}$ = 11.5 Hz, C$H_2$Bn), 4.62 (1H, d, $J_{gem}$ = 11.5 Hz, C$H_2$Bn), 4.59 (1H, d, $J_{gem}$ = 11.5 Hz, C$H_2$Bn), 4.55 (1H, d, $J_{gem}$ = 11.5 Hz, C$H_2$Bn), 4.36 (1H, d, $J_{2',3'}$ = 4.5 Hz, H3′), 4.22 (1H, m, $J_{2',8'}$ = 4.0 Hz, $J_{OH,8'}$ = 11.5 Hz, H8′), 4.03 (1H, d, $J_{OH,8'}$ = 11.5 Hz, 8′-OH), 3.77 (1H, d, $J_{gem}$ = 11.0 Hz, H5′), 3.59 (1H, d, $J_{gem}$ = 11.0 Hz, H5″), 2.82 (1H, t, $J_{2',8'}$ = 4.0 Hz, $J_{2',3'}$ = 4.5 Hz, H2′), 2.03 (2H, m, H7′ and H6′), 1.91 (1H, m, H7″), 1.49 (3H, d, $J_{6,CH_3}$ = 1.0 Hz, thymine-C$H_3$), 1.43 (1H, m, H6″). $^{13}$C NMR (125 MHz, $CDCl_3$) $\delta$ 163.7 (C4), 149.9 (C2), 137.1, 136.4 (2 × $C_{ipso}$-Bn), 135.9 (C6), 128.7−127.9 (aromatic), 109.4 (C5), 85.4 (C1′), 84.5 (C4′), 75.4 (C3′), 74.0, 73.6 (2 × C$H_2$Bn), 70.4 (C5′), 68.7 (C8′), 46.2 (C2′), 27.3 (C7′), 23.5 (C6′), 11.9 (C$H_3$-thymine). MALDI-TOF $m/z$ [$C_{27}H_{30}N_2O_6$ + Na]$^+$ found 501.200, calcd 501.200. **20b:** $^1$H NMR (500 MHz, $CDCl_3$) $\delta$ 8.05 (1H, s, H6), 7.35−7.18 (10H, m, aromatic), 6.08 (1H, s, H1′), 4.77 (1H, d, $J_{gem}$ = 12.0 Hz, C$H_2$Bn), 4.60 (1H, d, $J_{gem}$ = 12.0 Hz, C$H_2$Bn), 4.55 (2H, d, $J_{gem}$ = 12.0 Hz, 2 × C$H_2$Bn), 4.39 (1H, s, H3′), 4.37 (1H, m, H8′), 3.69 (1H, d, $J_{gem}$ = 11.0 Hz, H5′), 3.55 (1H, d, $J_{gem}$ = 11.0 Hz, H5″), 3.08 (1H, s, H2′), 2.04 (1H, m, H7′), 1.85 (1H, ddd, H6′), 1.62 (1H, m, H7″), 1.41 (1H, dd, H6″), 1.39 (3H, d, $J_{6,CH_3}$ = 1.0 Hz, thymine-C$H_3$). $^{13}$C NMR (125 MHz, $CDCl_3$) $\delta$ 164.5 (C4), 151.0 (C2), 138.1, 137.5 (2 × $C_{ipso}$-Bn), 136.7 (C6), 128.6−127.3 (aromatic), 108.8 (C5), 84.4 (C4′), 84.3 (C1′), 74.3 (C3′), 73.5, 71.9 (2 × C$H_2$Bn), 70.2 (C5′), 64.3 (C8′), 49.1 (C2′), 26.3 (C7′), 26.1 (C6′), 12.2 (C$H_3$-thymine). MALDI-TOF $m/z$ [$C_{27}H_{30}N_2O_6$ + H]$^+$ found 479.221, calcd 479.218.

**(1*R*,3*R*,4*R*,5*S*,8*S*)-8-Benzyloxy-1-benzyloxymethyl-5-(4-methyl-benzoate)-3-(thymin-1-yl)-2-oxa-bicyclo[3.2.1]octane (21a).** Compound **20a** (72 mg, 0.150 mmol) was dissolved in dry pyridine (3 mL) and the solution was cooled to 0 °C, then toluoyl chloride (0.1 mL, 0.760 mmol) was added. The mixture was allowed to warm to room temperature followed by stirring at this temperature overnight. Then the reaction was quenched with saturated $NaHCO_3$ solution. The aqueous layer was exacted with $CH_2Cl_2$ three times. The combined organic layer was dried over $MgSO_4$ and concentrated. The residue was chromatographed on silica gel (0.8−1.2% methanol in $CH_2Cl_2$, v/v) to obtain **21a** (81 mg, 90.0%) as a white foam. $^1$H NMR (500 MHz, $CDCl_3$) $\delta$ 8.19 (1H, s, H3), 8.04 (1H, s, H6), 7.79−6.98 (14H, m, aromatic), 5.73 (1H, s, H1′), 5.53 (1H, t, $J_{2',8'}$ = 4.0 Hz, $J_{7',8'}$ = 5.0 Hz, H8′), 4.72 (1H, d, $J_{gem}$ = 12.0 Hz, C$H_2$Bn), 4.60 (1H, d, $J_{gem}$ = 11.5 Hz, C$H_2$Bn), 4.55 (1H, d, $J_{gem}$ = 11.5 Hz, C$H_2$Bn), 4.48 (1H, d, $J_{gem}$ = 12.0 Hz, C$H_2$Bn), 4.23 (1H, d, $J_{2',3'}$ = 4.5 Hz, H3′), 3.78 (1H, d, $J_{gem}$ = 11.0 Hz, H5′), 3.66 (1H, d, $J_{gem}$ = 11.0 Hz, H5″), 3.10 (1H, t, $J_{2',8'}$ = 4.0 Hz, $J_{2',3'}$ = 4.5 Hz, H2′), 2.34 (3H, s, Tol-C$H_3$), 2.30 (1H, ddd, $J_{6',7''}$ = 5.5 Hz, $J_{6',7'}$ = 12.5 Hz, $J_{6',6''}$ = 13.0 Hz, H6′), 2.15 (1H, m, $J_{7',8'}$ = 5.0 Hz, $J_{6'',7'}$ = 6.0 Hz, $J_{6',7'}$ = 12.5 Hz, $J_{7',7''}$ = 15.5 Hz, H7′), 1.42 (1H, dd, $J_{6',7''}$ = 5.5 Hz, $J_{7',7''}$ = 15.5 Hz, H7″), 1.41 (1H, dd, $J_{6'',7'}$ = 6.0 Hz, $J_{6',6''}$ = 13.0 Hz, H6″), 1.41 (3H, s, thymine-C$H_3$). $^{13}$C NMR (125 MHz, $CDCl_3$) $\delta$ 166.1 (C═O), 163.6 (C4), 149.8 (C2), 143.5 ($C_{ipso}$-Tol), 137.6, 137.3 (2 × $C_{ipso}$-Bn), 136.0 (C6), 129.7−127.2 (aromatic), 109.3 (C5), 85.8 (C1′), 84.8 (C4′), 73.6 (C$H_2$Bn), 73.1 (C3′), 72.5 (C$H_2$Bn), 70.3 (C5′), 69.4 (C8′), 44.7(C2′), 24.3 (C7′), 24.0 (C6′), 21.6 (C$H_3$-Tol), 11.8 (C$H_3$-thymine). MALDI-TOF $m/z$ [$C_{35}H_{36}N_2O_7$ + H]$^+$ found 597.263, calcd 597.260.

**(1*R*,3*R*,4*R*,5*S*,8*S*)-8-Benzyloxy-1-benzyloxymethyl-5-((methylthio)thiocarbonyl)oxy-3-(thymin-1-yl)-2-oxa-bicyclo[3.2.1]octane (23).** To a solution of **20a** (77 mg, 0.161 mmol) in dry THF (3 mL) was added 60% NaH (32 mg, 1.808 mmol) at 0 °C. After the solution was stirred at room temperature for 1 h, $CS_2$ (89 $\mu$L, 1.62 mmol) was added to the suspension at 0 °C, and the resulting mixture was stirred at 40 °C for 4 h. The solution became clear and was cooled by ice to which methyl iodide (65 $\mu$L, 1.05 mmol) was added dropwise at 0 °C followed by stirring at room temperature overnight. The reaction was quenched by chilled water, then extracted with ethyl acetate three times. The combined organic layer was dried over $MgSO_4$ and evaporated. The residue was chromatographed over silica gel

(0.5−0.7% methanol in $CH_2Cl_2$, v/v) to give **23** (48 mg, 52.7%) as a yellow foam. $^1$H NMR (500 MHz, $CDCl_3$) $\delta$ 8.04 (1H, d, $J_{6,CH_3}$ = 1.5 Hz, H6), 8.02 (1H, s, H3), 7.37−7.25 (10H, m, aromatic), 6.03 (1H, t, $J_{2',8'}$ = 3.5 Hz, H8′), 5.72 (1H, s, H1′), 4.80 (1H, d, $J_{gem}$ = 12.0 Hz, C$H_2$Bn), 4.60 (1H, d, $J_{gem}$ = 11.5 Hz, C$H_2$Bn), 4.56 (1H, d, $J_{gem}$ = 11.5 Hz, C$H_2$Bn), 4.45 (1H, d, $J_{gem}$ = 12.0 Hz, C$H_2$Bn), 4.24 (1H, d, $J_{2',3'}$ = 4.5 Hz, H3′), 3.77 (1H, d, $J_{gem}$ = 11.0 Hz, H5′), 3.65 (1H, d, $J_{gem}$ = 11.0 Hz, H5″), 3.23 (1H, t, $J_{2',8'}$ = 3.5 Hz, $J_{2',3'}$ = 4.5 Hz, H2′), 2.50 (3H, s, $SCH_3$), 2.16 (3H, m, H6′, H7′ and H7″), 1.43 (1H, m, H6″), 1.42 (3H, d, $J_{6,CH_3}$ = 1.5 Hz, thymine-C$H_3$). $^{13}$C NMR (125 MHz, $CDCl_3$) $\delta$ 215.1 (C═S), 163.5 (C4), 149.7 (C2), 137.7, 137.3 (2 × $C_{ipso}$-Bn), 135.9 (C6), 128.7−127.6 (aromatic), 109.4 (C5), 85.5 (C1′), 85.0 (C4′), 78.1 (C8′), 73.7 (C$H_2$Bn), 72.6 (C3′), 72.4 (C$H_2$Bn), 70.2 (C5′), 44.4 (C2′), 24.0 (C7′), 23.8 (C6′), 19.0 ($SCH_3$), 11.8 (C$H_3$-thymine). MALDI-TOF $m/z$ $[C_{29}H_{32}N_2O_6S_2 + H]^+$ found 569.180, calcd 569.177.

**(1*R*,3*R*,4*R*,8*S*)-8-Benzyloxy-1-benzyloxymethyl-3-(thymin-1-yl)-2-oxa-bicyclo[3.2.1]octane (24). 23** (64 mg, 0.112 mmol) was dissolved in dry toluene (5 mL) and the solution was purged with dry nitrogen for 30 min. AIBN (9 mg, 0.034 mmol) and $Bu_3SnH$ (91 $\mu$L, 0.338 mmol) were added to the mixture followed by reflux for 1.5 h. The mixture was cooled to room temperature and solvent was evaporated. The residue was subject to short column chromatography over silica gel (0.5−0.7% methanol in $CH_2Cl_2$, v/v) to obtain **24** (38 mg, 73.5%) as a white foam. $^1$H NMR (500 MHz, $CDCl_3$) $\delta$ 8.09 (1H, d, $J_{6,CH_3}$ = 1.0 Hz, H6), 7.98 (1H, s, H3), 7.49−7.30 (10H, m, aromatic), 5.84 (1H, s, H1′), 4.63 (1H, d, $J_{gem}$ = 11.5 Hz, C$H_2$Bn), 4.61 (1H, d, $J_{gem}$ = 11.5 Hz, C$H_2$Bn), 4.56 (1H, d, $J_{gem}$ = 11.5 Hz, C$H_2$Bn), 4.48 (1H, d, $J_{gem}$ = 11.5 Hz, C$H_2$Bn), 4.18 (1H, d, $J_{2',3'}$ = 5.0 Hz, H3′), 3.71 (1H, d, $J_{gem}$ = 10.5 Hz, H5′), 3.57 (1H, d, $J_{gem}$ = 10.5 Hz, H5″), 2.60 (1H, m, $J_{2',3'}$ = 5.0 Hz, H2′), 1.94 (1H, m, H8′), 1.87 (1H, m, H6′), 1.74 (3H, m, H8″, H7′ and H7″), 1.46 (3H, d, $J_{6,CH_3}$ = 1.0 Hz, thymine-C$H_3$), 1.36 (1H, m, H6″). $^{13}$C NMR (125 MHz, $CDCl_3$) $\delta$ 163.7 (C4), 149.9 (C2), 137.8, 137.5 (2 × $C_{ipso}$-Bn), 136.5 (C6), 128.6−127.4 (aromatic), 109.1 (C5), 87.5 (C1′), 85.4 (C4′), 73.5 (C$H_2$Bn), 73.0 (C3′), 71.7 (C$H_2$Bn), 70.7 (C5′), 42.9 (C2′), 26.9 (C6′), 20.7 (C8′), 17.7 (C7′), 11.8 (C$H_3$-thymine). MALDI-TOF $m/z$ $[C_{27}H_{30}N_2O_5 + H]^+$ found 463.226, calcd 463.223.

**(1*R*,3*R*,4*R*,5*S*,8*S*)-8-Benzyloxy-1-benzyloxymethyl-5-hydroxy-5-methyl-3-(thymin-1-yl)-2-oxa-bicyclo[3.2.1]octane (26). 19** (100 mg, 0.21 mmol) was dissolved in dry THF (3 mL) and the mixture was cooled to −78 °C, then MeLi (393 $\mu$L, 1.6 M in $Et_2O$, 0.63 mmol) was added dropwise. After the solution was stirred at −78 to −65 °C for 10 h, the reaction was quenched by addition of saturated $NH_4Cl$ solution. Upon warming to room temperature, the mixture was diluted with EtOAc and $H_2O$. The aqueous layer was extracted with EtOAc three times. The combined organic layers were dried by $MgSO_4$, and then evaporated to dryness. **26** (60 mg, 58%) was obtained by chromatography on silica gel (0.5−3% methanol in $CH_2Cl_2$, v/v), and starting material (30 mg, 30%) was recovered. $^1$H NMR (500 MHz, $CDCl_3$) $\delta$ 8.35 (1H, s, H3), 8.06 (1H, d, $J_{6,CH_3}$ = 1.5 Hz, H6), 7.40−7.28 (10H, m, aromatic), 5.66 (1H, s, H1′), 4.90 (1H, s, OH), 4.76 (1H, d, $J_{gem}$ = 11.0 Hz, C$H_2$Bn), 4.62 (1H, d, $J_{gem}$ = 11.5 Hz, C$H_2$Bn), 4.58 (1H, d, $J_{gem}$ = 11.0 Hz, C$H_2$Bn), 4.56 (1H, d, $J_{gem}$ = 11.5 Hz, C$H_2$Bn), 4.35 (1H, d, $J_{2',3'}$ = 4.5 Hz, H3′), 3.77 (1H, d, $J_{gem}$ = 11.0 Hz, H5′), 3.60 (1H, d, $J_{gem}$ = 11.0 Hz, H5″), 2.48 (1H, d, $J_{2',3'}$ = 4.5 Hz, H2′), 1.98 (1H, ddd, $J_{6',7''}$ = 6.0 Hz, $J_{6',7'}$ = 13.0 Hz, $J_{6',6''}$ = 13.0 Hz, H6′), 1.82 (1H, ddd, $J_{7',6''}$ = 6.0 Hz, $J_{6',7'}$ = 13.0 Hz, $J_{7',7''}$ = 14.0 Hz, H7′), 1.75 (1H, dd, $J_{6',7''}$ = 6.0 Hz, $J_{7',7''}$ = 14.0 Hz, H7″), 1.50 (3H, d, $J_{6,CH_3}$ = 1.5 Hz, thymine-C$H_3$), 1.44 (4H, m, $J_{6'',7'}$ = 6.0 Hz, $J_{6',6''}$ = 13.0 Hz, C$H_3$ and H6″). $^{13}$C NMR (125 MHz, $CDCl_3$) $\delta$ 162.7 (C4), 148.8 (C2), 136.1, 135.1 (2 × $C_{ipso}$-Bn), 135.0 (C6), 127.7−127.0 (aromatic), 108.3 (C5), 84.9 (C1′), 82.6 (C4′), 74.7 (C3′), 73.1, 72.6 (2 × C$H_2$Bn), 71.2 (C8′), 69.1 (C5′), 49.3 (C2′), 32.2 (C7′), 26.6 (8′-C$H_3$), 23.4 (C6′), 10.9 (C$H_3$-thymine). MALDI-TOF $m/z$ $[C_{28}H_{32}N_2O_6 + H]^+$ found 493.235, calcd 493.234.

**(1*R*,3*R*,4*R*,5*S*,8*S*)-8-Benzyloxy-1-benzyloxymethyl-5-methoxalyloxy-5-methyl-3-(thymin-1-yl)-2-oxa-bicyclo[3.2.1]octane (27). 26** (60 mg, 0.12 mmol) was dissolved in dry pyridine (1.5 mL) to which methyl oxalyl chloride (90 $\mu$L, 0.974 mmol) was added. The mixture was stirred at 40 °C overnight. After evaporation of solvent, the residue obtained was dissolved in $CH_2Cl_2$, washed with saturated $NaHCO_3$ solution, dried over $MgSO_4$, and evaporated. The residue was purified by column chromatography on silica gel (0.5−1% methanol in $CH_2Cl_2$, v/v) to give **27** (61 mg, 87%). $^1$H NMR (500 MHz, $CDCl_3$): $\delta$ 8.68 (1H, s, NH), 8.02 (1H, d, $J_{6,CH_3}$ = 1.5 Hz, H6), 7.35−7.23 (10H, m, aromatic), 5.70 (1H, s, H1′), 4.63 (1H, d, $J_{gem}$ = 11.5 Hz, C$H_2$Bn), 4.57 (1H, d, $J_{gem}$ = 11.5 Hz, C$H_2$Bn), 4.53 (1H, d, $J_{gem}$ = 11.5 Hz, C$H_2$Bn), 4.48 (1H, d, $J_{gem}$ = 11.5 Hz, C$H_2$Bn), 4.23 (1H, d, $J_{2',3'}$ = 4.5 Hz, H3′), 3.77 (1H, d, $J_{gem}$ = 11.0 Hz, H5′), 3.59 (1H, d, $J_{gem}$ = 11.0 Hz, H5″), 3.55 (1H, d, $J_{2',3'}$ = 4.5 Hz, H2′), 2.22 (2H, m, H6′ and H7′), 1.83 (1H, m, H7″), 1.79 (3H, s, 8′-C$H_3$), 1.46 (3H, d, $J_{6,CH_3}$ = 1.5 Hz, thymine-C$H_3$), 1.43 (1H, dd, H6″). $^{13}$C NMR (125 MHz, $CDCl_3$) $\delta$ 162.8 (C4), 157.2, 155.7 (oxalyl C═O), 148.9 (C2), 136.4, 136.0 (2 × $C_{ipso}$-Bn), 134.8 (C6), 127.7−126.4 (aromatic), 108.5 (C5), 84.5 (C1′), 83.2 (C8′), 82.7 (C4′), 73.6 (C3′), 73.0, 72.6 (2 × C$H_2$Bn), 69.1 (C5′), 51.9 ($OCH_3$), 46.8 (C2′), 31.0 (C7′), 23.7 (C6′), 22.9 (8′-C$H_3$), 10.9 (C$H_3$-thymine). MALDI-TOF $m/z$ $[C_{31}H_{34}N_2O_9 + H]^+$ found 579.235, calcd 579.234.

**General Procedure for Phosphoramidite Synthesis.** DIPEA (5 equiv) and 2-cyanoethyl-*N*,*N*-diisopropylphosphoramidochloridite (3 equiv) were added dropwise to a solution of substrate (1 equiv) in dry $CH_2Cl_2$ in an ice bath. The reaction was allowed to warm to room temperature and stirred at this temperature for 3 h (overnight for **22a**). The reaction was quenched with dry methanol followed by stirring over 15 min. Then the mixture was diluted with ethyl acetate and washed with saturated $NaHCO_3$ solution. The organic layer was dried over $MgSO_4$ and concentrated. The residue was chromatographed on silica gel to obtain the corresponding phosphoramidite, which was first precipitated in *n*-hexane then dried over $P_2O_5$ under vacuum for 3 days before it was used for DNA synthesis.

**Oligonucleotide Synthesis and Purification.** All AONs were synthesized with an automated DNA/RNA synthesizer based on phosphoramidite chemistry. For native A, G, and C building blocks, fast deprotecting phosphoramidites (Ac for C, *i*Pr-Pac for G, Pac for A) were used. Standard DNA synthesis reagents and cycle were used except that 0.25 M 5-ethylthio-1*H*-tetrazole was used as the activator and $Tac_2O$ as the cap A. For incorporating modified nucleotides, extended coupling time (10 min compared to 25 s for native nucleotides, 15 min for **30a**) was used. For AONs **2**−**9** the protection was performed in 33% aqueous ammonia at room temperature overnight. For AONs **10**−**13**, **14**−**17**, and **18**−**21** the protection was performed in 33% aqueous ammonia at 55 °C for 3, 2, and 1 day, respectively. After deprotection, all crude oligos were purified by denaturing PAGE (20% polyacrylamide with 7 M urea), extracted with 0.3 M NaOAc, and desalted with a C-18 reverse phase cartridge to give AONs in >99% purity, and correct masses have been obtained by MALDI-TOF mass spectroscopy for each of them (Table SII 1,Supporting Information).

**UV Melting Experiments.** Determination of the $T_m$ of the AON:RNA hybrids or AON:DNA duplex was carried out in the following buffer: 60 mM Tris-HCl (pH 7.5), 60 mM KCl, 0.8 mM $MgCl_2$. Absorbance was monitored at 260 nm in the temperature range from 20 to 70 °C, using an UV spectrophotometer equipped with a Peltier temperature programmer with the heating rate of 1 deg/min. Prior to measurements, the samples (1 $\mu$M of AON and 1 $\mu$M cDNA or RNA mixture) were preannealed by heating to 80 °C for 5 min followed by slow cooling to 21 °C and 30 min of equilibration at this temperature. The value of $T_m$ is the average of two or three independent measurements. If error of the first two measurements is > ±0.3 °C,

the third measurement was carried out to check if the error is indeed within ±0.3 °C, otherwise it is repeated again.

**$^{32}$P Labeling of Oligonucleotides.** The oligoribonucleotides and oligodeoxyribonucleotides were 5′-end labeled with $^{32}$P, using T4 polynucleotide kinase, [$\gamma$-$^{32}$P]ATP, and the standard protocol. Labeled AONs and the target RNA were purified by QIAquick Nucleotide Removal Kit, and specific activities were measured with a Beckman LS 3801 counter.

**SVPDE Degradation Studies.** Stability of the AONs toward 3′-exonucleases was tested by using phosphodiesterase I from *Crotalus adamanteus* (obtained from USB corporation, Cleveland, Ohio). All reactions were performed at 3 $\mu$M DNA concentration (5′-end $^{32}$P labeled with specific activity 80 000 cpm) in 100 mM Tris-HCl (pH 8.0) and 15 mM $MgCl_2$ at 21 °C. An exonuclease concentration of 6.7 ng/$\mu$L was used for digestion of oligonucleotides. Total reaction volume was 30 $\mu$L. Aliquots (3 $\mu$L) were taken at proper time points and quenched by addition of stop solution (4 $\mu$L) [containing 0.05 M EDTA, 0.05% (w/v) bromophenol blue, and 0.05% (w/v) xylene cyanole in 80% formamide]. Reaction progress was monitored by 20% denaturing (7 M urea) PAGE and autoradiography.

The total percentage of integrated AONs (13- and 14mer) was plotted against time points to give the digestion curve, and the pseudo-first-order reaction rate could be obtained by fitting curves to single-exponential decay functions.

**Stability Studies in Human Blood Serum.** AONs at 2 $\mu$M concentration (5′-end $^{32}$P labeled with specific activity 80 000 cpm) were incubated in 10 $\mu$L of human blood serum (male AB, obtained from Sigma-aldrich) at 21 °C (total reaction volume was 36 $\mu$L). Aliquots (3 $\mu$L) were taken at proper time points and quenched with 4 $\mu$L of stop solution [containing 0.05 M EDTA, 0.05% (w/v) bromophenol blue, and 0.05% (w/v) xylene cyanole in 80% formamide], resolved in 20% polyacrylamide denaturing (7 M urea) gel electrophoresis, and visualized by autoradiography.

**RNase H Digestion Assay.** Target 0.1 $\mu$M RNA (specific activity 80 000 cpm) and AON (2 $\mu$M) were incubated in a buffer containing 20 mM Tris-HCl (pH 7.5), 20 mM KCl, 10 mM $MgCl_2$, 0.1 mM EDTA, and 0.1 mM DTT at 21 °C in the presence of 0.08 U *E. coli* RNase H (obtained from USB corporation, Cleveland, Ohio). Prior to the addition of the enzyme, reaction components were preannealed in the reaction buffer by heating at 80 °C for 5 min followed by slow cooling to 21 °C and 30 min equilibration at this temperature. Total reaction volume was 30 $\mu$L. Aliquots of 3 $\mu$L were removed after 5, 10, 15, 30, and 60 min, and the reactions were terminated by mixing with stop solution [containing 0.05 M EDTA, 0.05% (w/v) bromophenol blue, and 0.05% (w/v) xylene cyanole in 80% formamide]. The samples were subjected to 20% 7 M urea PAGE and visualized by autoradiography. Pseudo-first-order reaction rates could be obtained by fitting the digestion curves to single-exponential decay functions.

**Acknowledgment.** Generous financial support from the Swedish Natural Science Research Council (Vetenskapsradet), the Swedish Foundation for Strategic Research (Stiftelsen för Strategisk Forskning), and the EU-FP6 funded RIGHT project (Project no. LSHB-CT-2004-005276) is gratefully acknowledged. Jianfeng Xu and Mansoureh Karimiahmadabadi have equally contributed in this work.

**Supporting Information Available:** $^{1}$H, $^{13}$C, $^{31}$P, COSY, HMQC, and HMBC of all carba-ENA derivatives (SI part I); 1D NOE spectra of key intermediates **14**, **20a**, **21b**, **26**, and **28**, decoupling experiments of key intermediates **14**, **16b**, and **21a**/**b** (SI part II); denaturing PAGE analysis of the SVPDE degradation of AONs with modified carba-LNA analogues; discussion about stability of carba-ENA analogues-modified AONs in blood serum; autoradiograms of 20% denaturing PAGE as well as degradation curves, showing the cleavage kinetics of target RNA in AON:RNA hybrid duplexes by *E. coli* RNase H1; all individual reaction steps, workup, and product characterization for the intermediates **21b**, **22a/b**, **25**, **28**, and **29**, ENA and the characterization for final amidites **18a/b**, **30a/b**, **31**, and **32** (SI part II). This material is available free of charge via the Internet at http://pubs.acs.org.